New Chapter in the hundred-year Saga of Gravitational Waves

Plamen Fiziev
Sofia University Foundation for
Theoretical and Computational Physics and Astrophysics
&
BLTF, JINR, Dubna

Seminar Talk, BAN, Sofia, 7 April 2014

Background Imaging of Cosmic Extragalactic Polarization (BICEP)

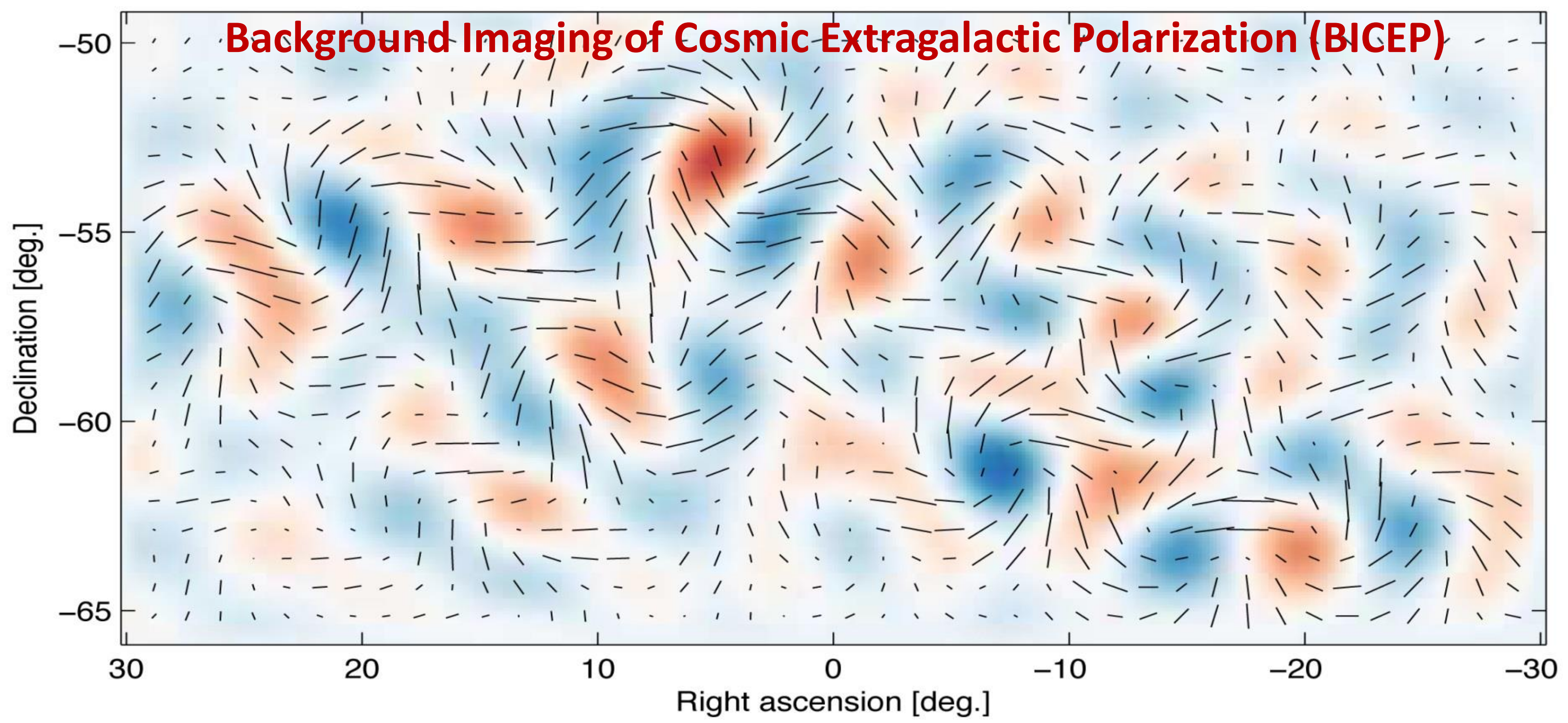

Predicted in 1916 by Albert Einstein to exist on the basis of his theory of general relativity, gravitational waves theoretically transport energy as gravitational radiation.

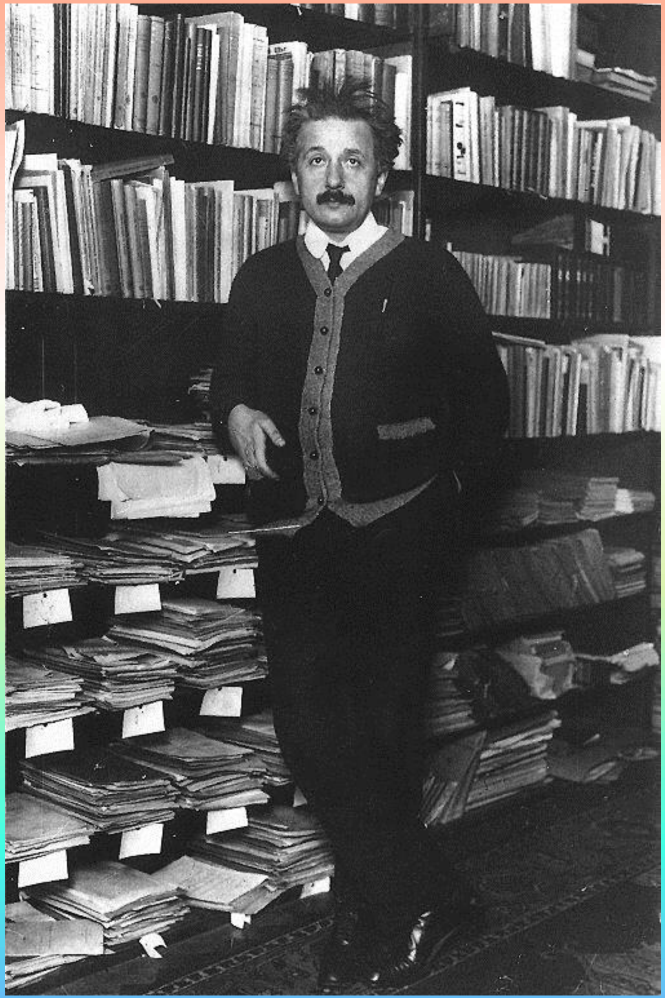

A. Einstein, Sitzungsber. preuss. Akad. Wiss.,
B. 1916, S.688; 1918,S. 154.

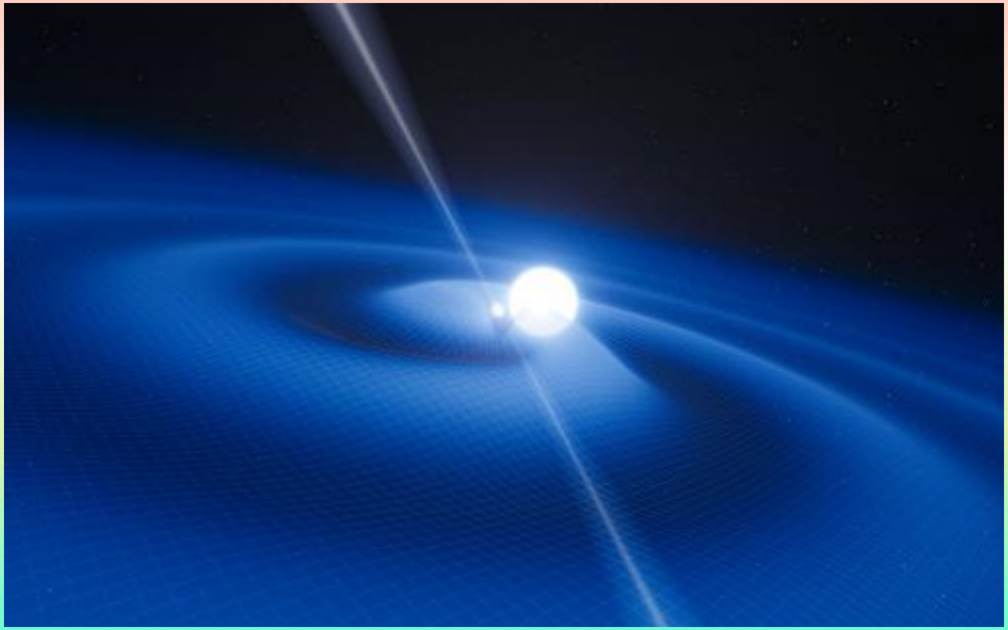

Remember that the basic PHYSICAL Einsten's idea inventing GR was the finite speed of spreading of gravity!
The geometry was only a tool!

Weak field approximation

$$g_{\mu\nu} = \eta_{\mu\nu} + h_{\mu\nu}, \quad h_{\mu\nu} \ll 1.$$

$$S_{\mu\nu} = T_{\mu\nu} - 1/2\, g_{\mu\nu} T^{\lambda}{}_{\lambda}$$

$$h_{\mu\nu}(x,t) = \frac{4G}{c^2} \int \frac{S_{\mu\nu}(x', t - \frac{|x-x'|}{c})}{|x-x'|}\, d^3x'$$

Flat waves: $h_{\mu\nu} = \varepsilon_{\mu\nu} \exp(ik_{\lambda}x^{\lambda}) + \varepsilon^{*}_{\mu\nu} \exp(-ik\lambda x^{\lambda})$.

Wave equation: $k^{\mu}k_{\mu} = 0$

Harmonic gauge: $k_{\mu}\varepsilon^{\mu}{}_{\nu} = 1/2\, k_{\nu}\varepsilon^{\mu}{}_{\mu} \qquad \varepsilon_{\mu\nu} = \varepsilon_{\nu\mu}$

Gauge transformations:

$$x'^{\mu} = x^{\mu} + \xi^{\mu}(x). \Rightarrow \quad h'_{\mu\nu} = h_{\mu\nu} - \xi_{\mu,\nu} - \xi_{\nu,\mu}$$

$$\varepsilon'_{\mu\nu} = \varepsilon_{\mu\nu} + k_{\mu}e_{\nu} + k_{\nu}e_{\mu}.$$

$$\xi^{\mu}(x) = i\, e_{\mu} e^{ikx} - i\, e^{*}_{\mu} e^{-ikx}$$

Flat GW along axes Oz:

$$k^3 = k^0 \equiv k(>0), \quad k^1 = k^2 = 0$$

$$h_{\mu\nu} = \begin{pmatrix} 0 & 0 & 0 & 0 \\ 0 & h_{11} & h_{12} & 0 \\ 0 & h_{12} & -h_{11} & 0 \\ 0 & 0 & 0 & 0 \end{pmatrix}$$

the graviton
is a particle with spin 2

Rotation around axes Oz:

only the two states $\varepsilon_{11} \pm i\varepsilon_{12}$ exist, with $J_z = \pm 2$

$$R(\theta) = \begin{pmatrix} \cos\theta & \sin\theta & 0 \\ -\sin\theta & \cos\theta & 0 \\ 0 & 0 & 1 \end{pmatrix} \Rightarrow \quad \varepsilon_{11}' - i\varepsilon_{12}' = e^{2i\theta}(\varepsilon_{11} - i\varepsilon_{12})$$

a state *with helicity* $h = 2$

$\varepsilon_{11} + i\,\varepsilon_{12}$ has helicity $h = -2$.

The two types of GW in GR:

$$V_{GW} = c$$

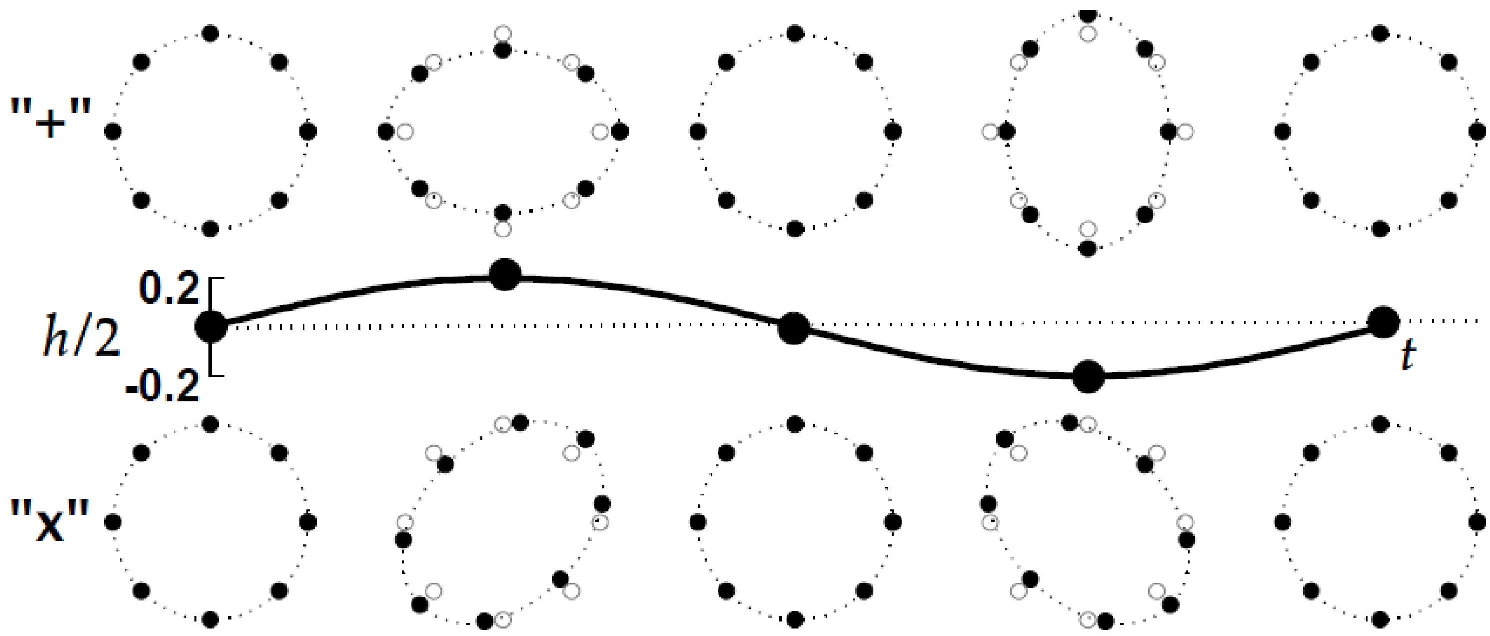

$$h = 2\frac{\delta \ell}{\ell}.$$

Polarization of GW in alternative theories of gravity

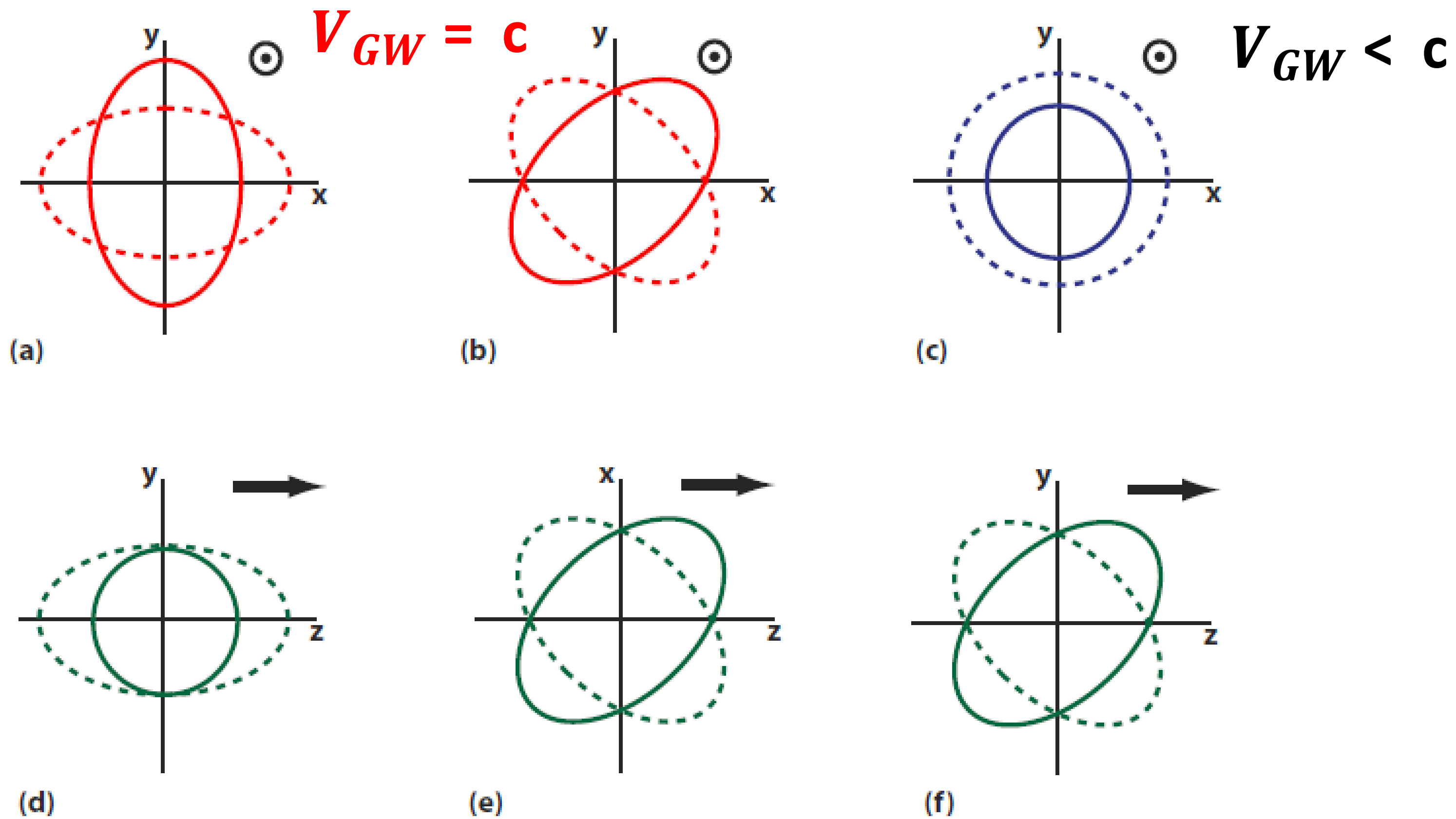

Figure 4: Effect of the six possible GW polarization modes on a ring of test particles. The GW propagates in the z-direction for the upper three transverse modes, and in the x-direction for the lower three longitudinal modes. Only modes (a) and (b) are possible in GR. Image reproduced by permission from [471].

Quadrupole character of GW (NASA Goddard)

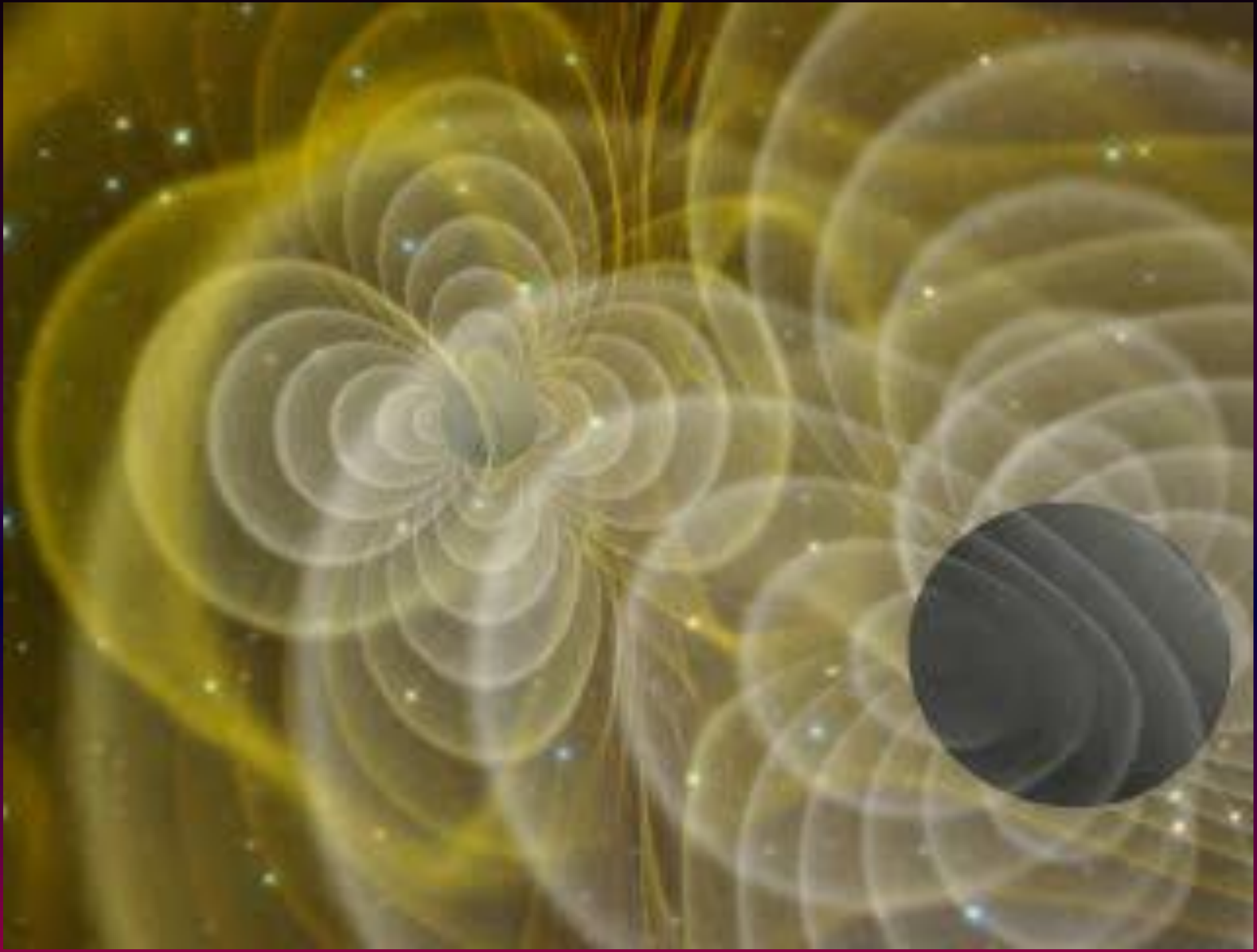

The first attempt for quantization of gravity

M. Bronstein, Sow. Phys., **3,** 73 (1933),
Quantization of gravitational waves

Proposed canonical quantization of week gravitational wave on flat background using relativistic invariant commutation relations and introducing for the first time gravitational quanta – gravitons, which meditate gravitational interaction between matter bodies.

1. **The Newton gravitational law is derived by calculating the exchange of gravitational quanta od spin 2.**
2. **The energy release by radiation of gravitational waves from matter bodies are calculated for the first time.**

The most important result of BICEP2, 2014
Confirmation of quantum nature of gravity: r > 0 at confidence level $7.0\,\sigma$

The first device used for unsuccessful search of gravitational waves and constructed by physicist Joseph Weber at the University of Maryland

Gravitational-Wave-Detector Events
Phys. Rev. Lett. **20**, 1307 – Published 3 June 1968, **J. Weber**

The **resonant-mass gravitational wave detector** was originally invented in **1959** by late Professor **Joseph Weber** in our group. The room-temperature detector developed by Weber in the 1960's laid the foundation for the later cryogenic antennas of improved sensitivity. In **1972**, **Ho Jung Paik**, then a graduate student at Stanford University, discovered the resonant transducer concept, which was generalized to a **multi-mode transducer** by Jean-Paul Richard in **1979**.

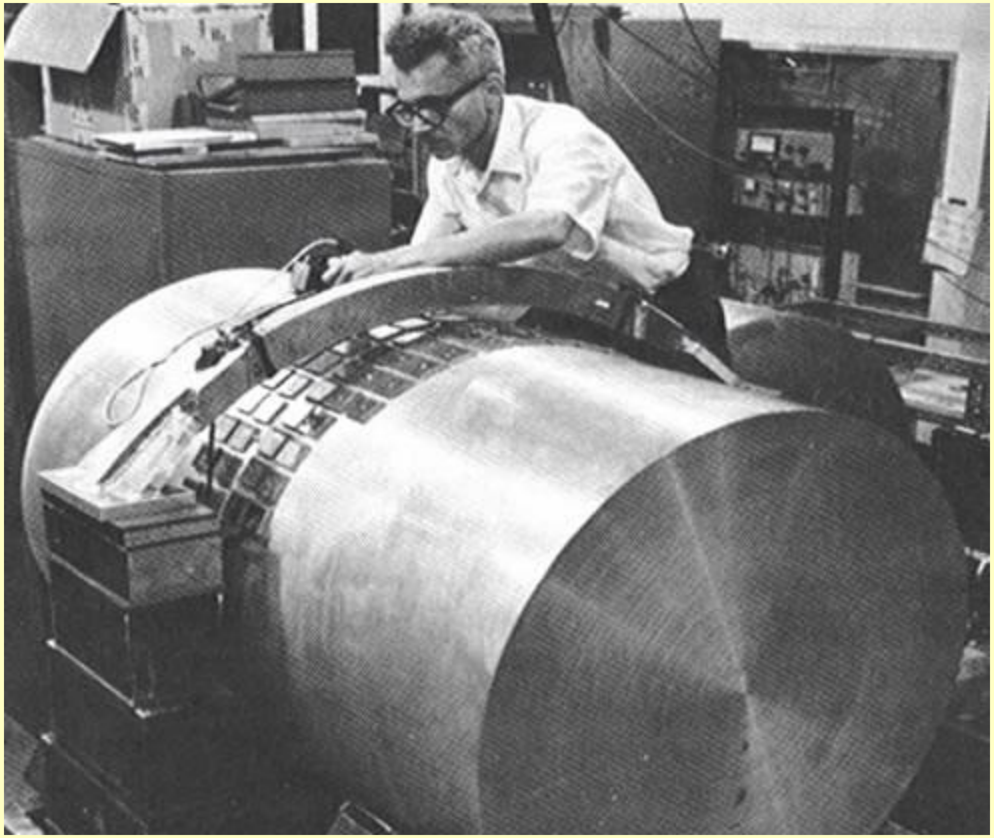

First indirect evidences for gravitational waves

$$P = \frac{\mathrm{d}E}{\mathrm{d}t} = -\frac{32}{5}\frac{G^4}{c^5}\frac{(m_1 m_2)^2(m_1+m_2)}{r^5}$$

$$\frac{\mathrm{d}\tau}{\mathrm{d}t} = (-2.422 \pm 0.006) \times 10^{-12}$$

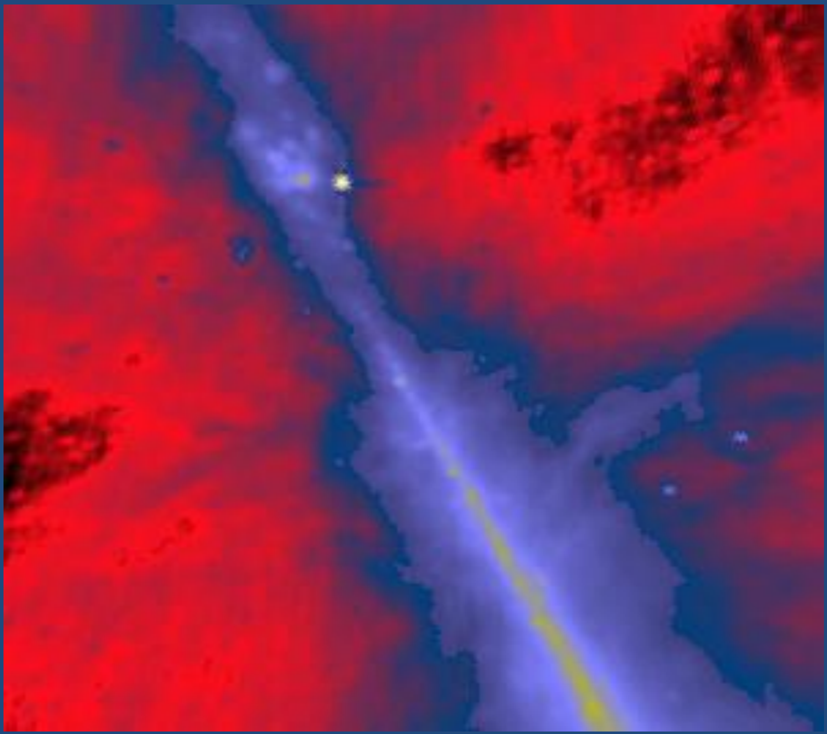

$$\frac{\mathrm{d}\tau}{\tau} = -\frac{48\pi}{5}\left(\frac{GM}{Rc^2}\right)^{5/2}$$

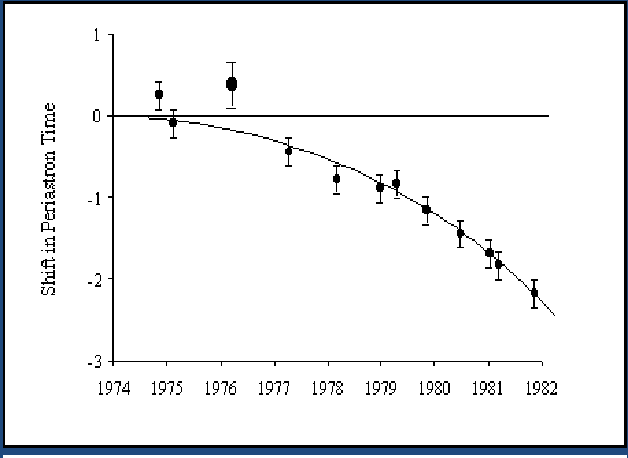

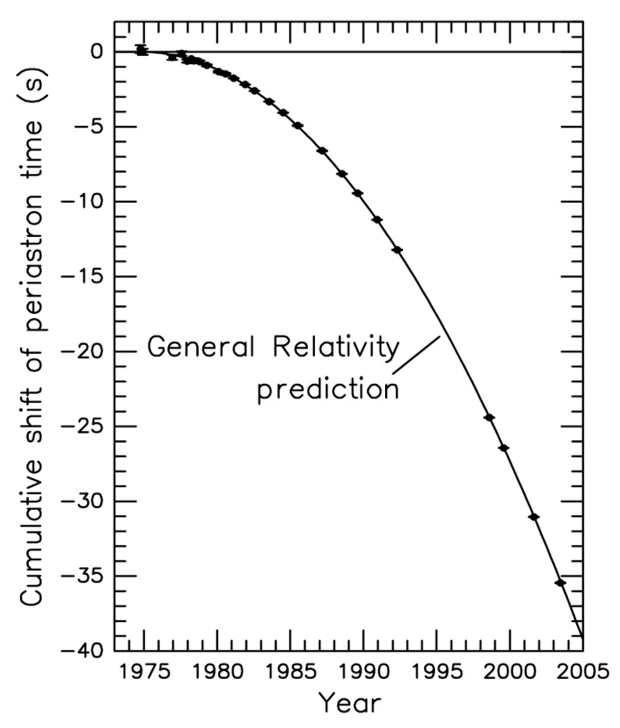

Indirect detection of gravitational waves
1993 Nobel Price: Hulst &Taylor

$$\dot{P}_{\mathrm{b\,GR}} = \frac{-192\pi M_{\mathrm{p}} M_{\mathrm{c}}}{5c^5 (M_{\mathrm{p}} + M_{\mathrm{c}})^{1/3}} \frac{1 + (73/24)e^2 + (37/96)e^4}{(1-e^2)^{7/2}} \left(\frac{2\pi G_{\mathrm{N}}}{P_{\mathrm{b}}}\right)^{5/3}$$

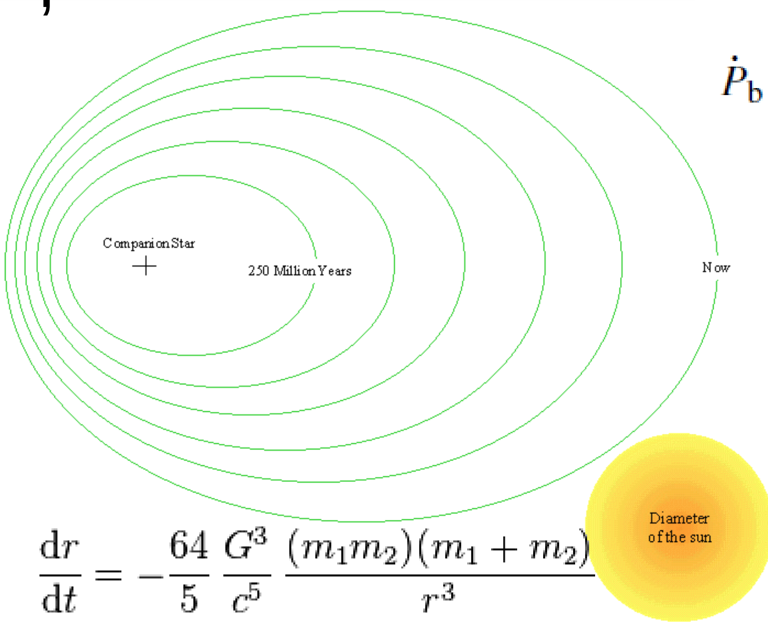

$$\frac{\mathrm{d}r}{\mathrm{d}t} = -\frac{64}{5}\frac{G^3}{c^5}\frac{(m_1 m_2)(m_1+m_2)}{r^3}$$

Table 1 PSR J0437–4715 physical parameters

Right ascension, α (J2000) ...	$04^h37^m15^s.7865145(7)$
Declination, δ (J2000)	$-47°15'08''.461584(8)$
μ_α (mas yr^{-1})	121.438(6)
μ_δ (mas yr^{-1})	-71.438(7)
Annual parallax, π (mas)	7.19(14)
Pulse period, P (ms)	5.757451831072007(8)
Reference epoch (MJD)	51194.0
Period derivative, $\dot{P}$ (10^{-20}) ..	5.72906(5)
Orbital period, P_b (days)	5.741046(3)
x (s)	3.36669157(14)
Orbital eccentricity, e	0.000019186(5)
Epoch of periastron, T_0 (MJD)	51194.6239(8)
Longitude of periastron, ω (°) .	1.20(5)
Longitude of ascension, Ω (°) .	238(4)
Orbital inclination, i (°)	42.75(9)
Companion mass, m_2 ($M_\odot$) ...	0.236(17)
$\dot{P}_b$(10^{-12})	3.64(20)
$\dot{\omega}$ (°yr^{-1})	0.016(10)

The pulsar's orbit is shrinking with time as shown in this diagram; currently, the orbit shrinks by about 3.1 mm per orbit.

The two stars should merge in about 300 million years from now.

The rate of decrease of orbital period is 76.5 microseconds per year, the rate of decrease of semimajor axis is 3.5 meters per year, and the calculated lifetime to final inspiral is 300,000,000 years.

Mass of companion 1.387 Msun Orbital period 7.751939106 hr
Eccentricity 0.617131
Semimajor axis 1,950,100 km
Periastron separation 746,600 km
Apastron separation 3,153,600 km
Orbital velocity of stars at periastron (relative to center of mass) 450 km/sec
Orbital velocity of stars at apastron (relative to center of mass) 110 km/sec

BH merger:

- The collision of two BH will produce a ringing single final BH (Stephen Hawking,+…)

From the ring-down waves we can infer the mass, the spin and surface area of the final BH.

- Kip Thorne, in The Future of Theoretical Physics and Cosmology, Cambridge, 2003:

"If the total area does not increase, Stephen is wrong, Einstein's GR laws are wrong, and we will have a great crisis in physics… Since the 1970's these remarkable predictions have remained untested. They seem to be an unequivocal consequence of Einstein's GR laws,

but relativity might be wrong or (much less likely)

we might be misinterpreting its mathematics."

BH merger (NR)

Several Orbits: NR is not what it was!

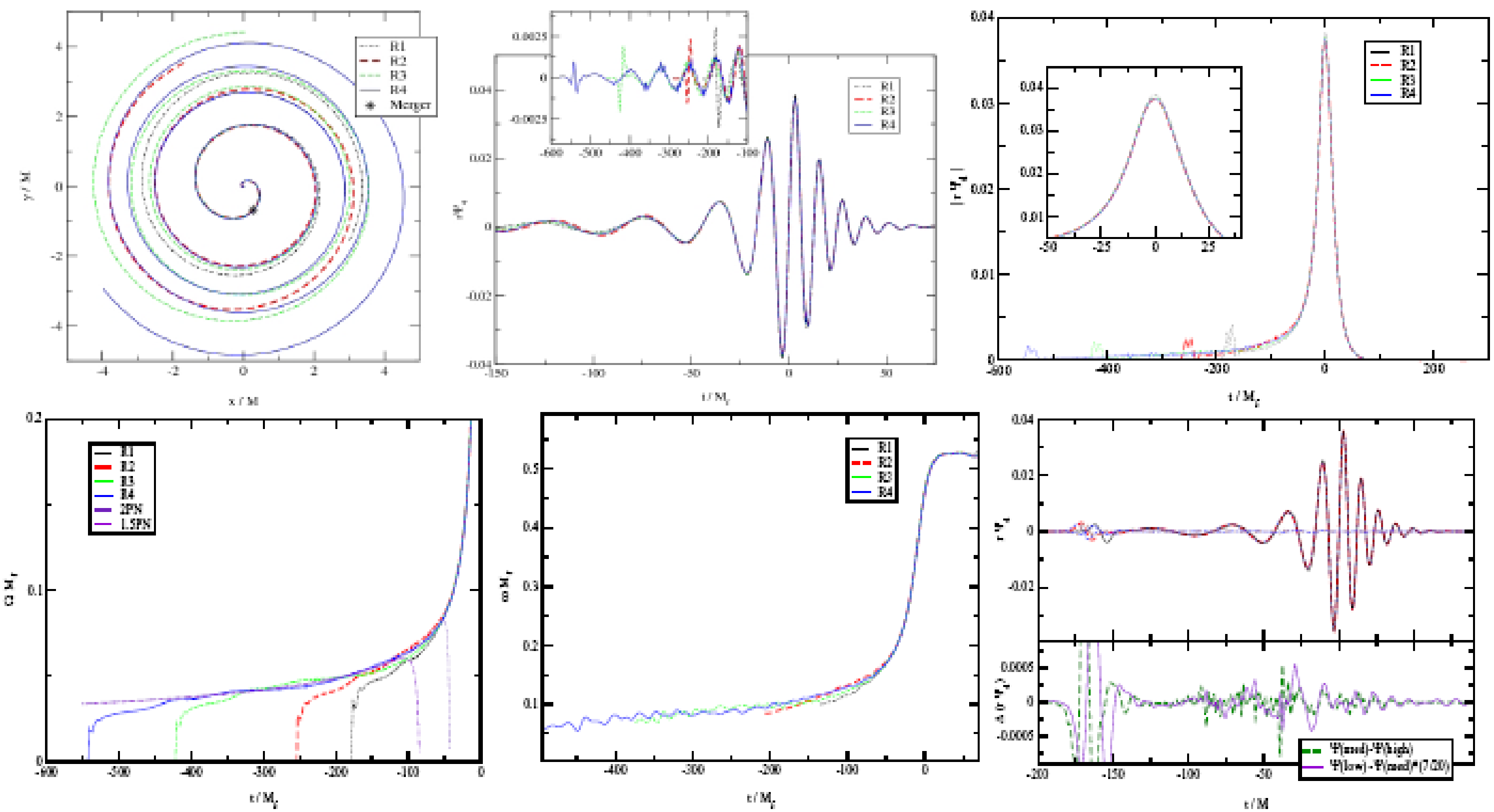

Figure: Success after 30 years: 4.2 Orbits and waveforms, NASA Goddard.

Radiated energy: $3.6 - 3.9\%$, final $a/M \approx 0.7$.

APJ 528: L17-L20, 2000

BLACK HOLE MERGERS IN THE UNIVERSE

we obtain the detection rate mentioned in § 1. For black hole binaries with $m_1 = m_2 = m_{\rm bh} = 10\ M_\odot$, we find $M_{\rm chirp} = 8.71\ M_\odot$, $R_{\rm eff} = 109$ Mpc, and a LIGO-I detection rate of about $1.7\ h^3\ {\rm yr}^{-1}$. For $h \sim 0.65$ (Jha et al. 1999), this results in about one detection event every 2 years. LIGO-II should become operational by 2007 and is expected to have $R_{\rm eff}$ about 10 times greater than LIGO-I, resulting in a detection rate 1000 times higher, ~ 1 event ${\rm day}^{-1}$.

Phys.Rev. D 77: 084002 (2008)

Fully General Relativistic Simulations of BH-NS Mergers

The overall rate estimates for BH-NS mergers observable by an advanced
LIGO detector typically fall in the range **R= 1 – 100 yr−1**

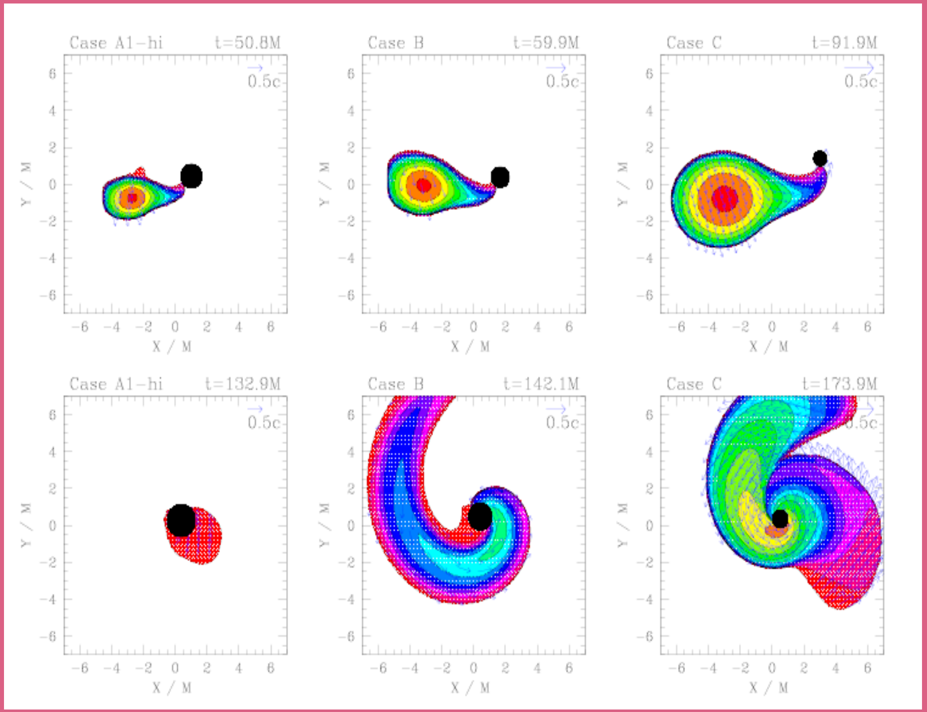

Detection of Gravitational Waves

Consider the effect of a wave on a ring of particles :

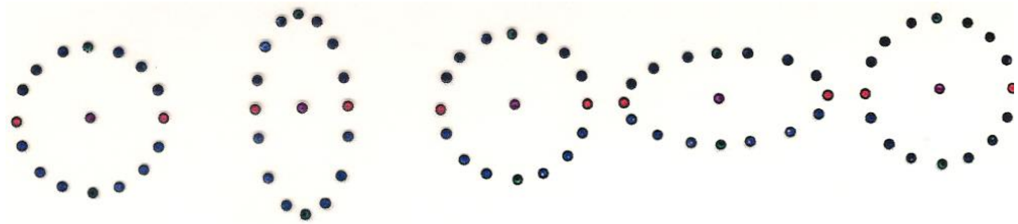

One cycle

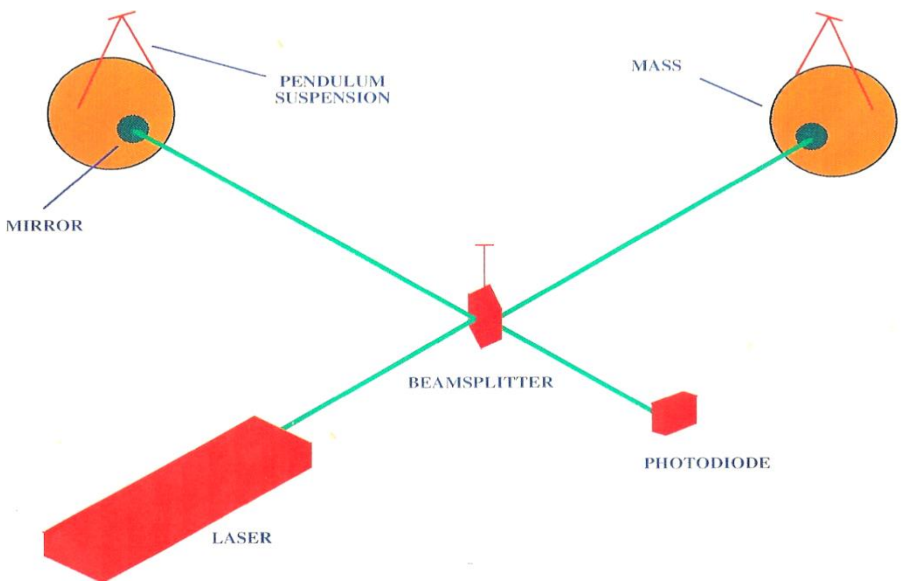

Michelson Interferometer

Gravitational waves have very weak effect:

expect movements of less than 10^{-18} m over 4km

Detection again

$$h \sim \frac{\Delta L}{L} \sim \frac{10^{-18}\,\mathrm{m}}{4\,\mathrm{km}}$$

wave amplitude

Interferometer

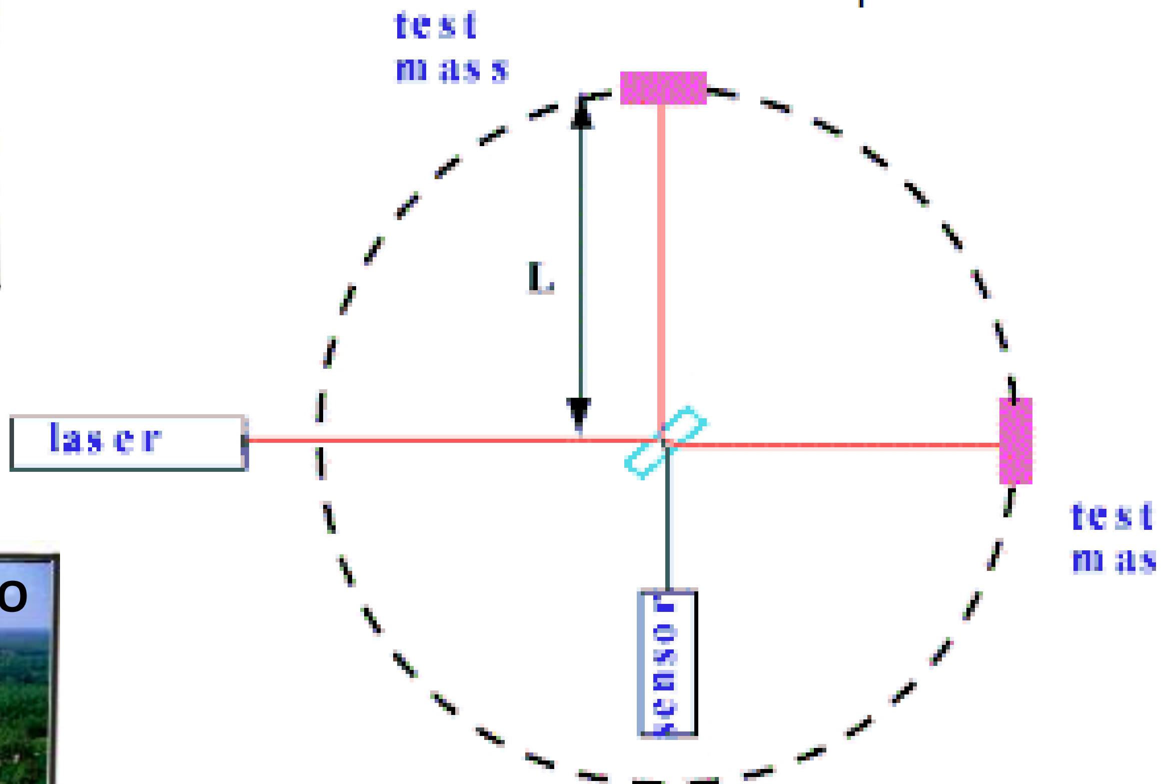

Interferometers - *international network*

'Simultaneously' detect signal (within msec)

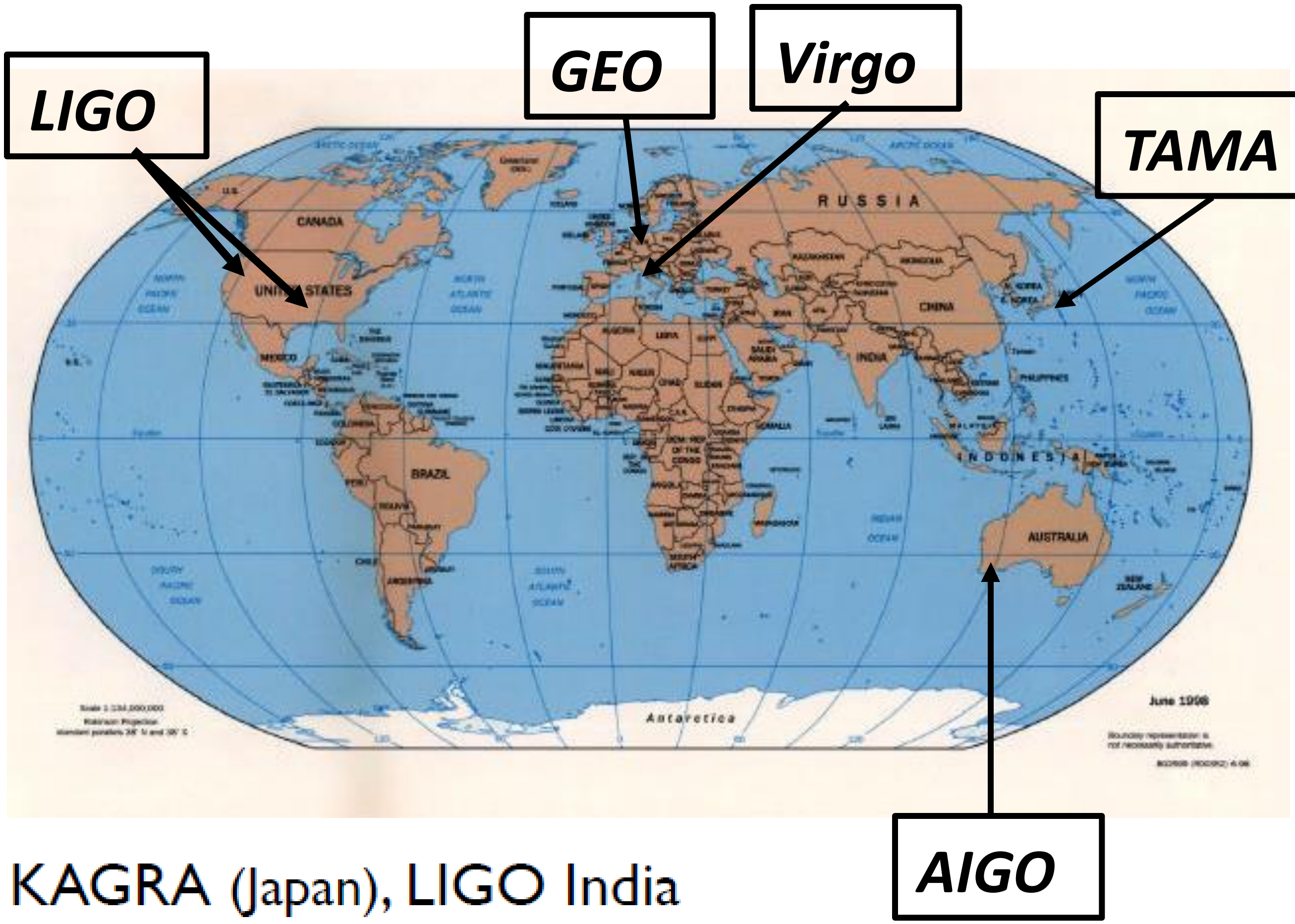

detection confidence

locate the sources

decompose the polarization of gravitational waves

KAGRA (Japan), LIGO India

2020

arXiv:1403.6639

March 27, 2014

SEARCH FOR GRAVITATIONAL WAVES ASSOCIATED WITH GAMMA-RAY BURSTS DETECTED BY THE INTERPLANETARY NETWORK

J. Aasi[1], B. P. Abbott[1], R. Abbott[1], T. Abbott[2], M. R. Abernathy[1], F. Acernese[3,4], K. Ackley[5], C. Adams[6],...

Collaboration of 138 Institutes ...

We present the results of a search for gravitational waves associated with **223 gamma-ray bursts (GRBs)** detected by **the InterPlanetary Network (IPN)** in 2005{2010 during LIGO's fith and sixth science runs and Virgo's first, second and third science runs.
The IPN satellites provide accurate times of the bursts and sky localizations that vary signicantly from degree scale to hundreds of square degrees.

We place lower bounds on the distance to the source in accordance with an optimistic assumption of gravitational-wave emission energy of 102 M at 150 Hz, and nd a median of 13Mpc. For the 27 short-hard GRBs we place 90% confidence exclusion
distances to two source models: a binary neutron star coalescence, with a median distance of 12Mpc, or the coalescence of a neutron star and black hole, with a median distance of 22Mpc.

No gravitational wave was detected
in coincidence with a GRB, and lower limits on the distance were set for each GRB for various gravitational-wave emission models.

My personal opinion:
The predicted sources simply do not exist!

GRB070201:

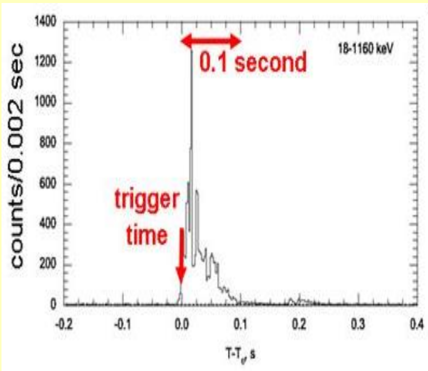

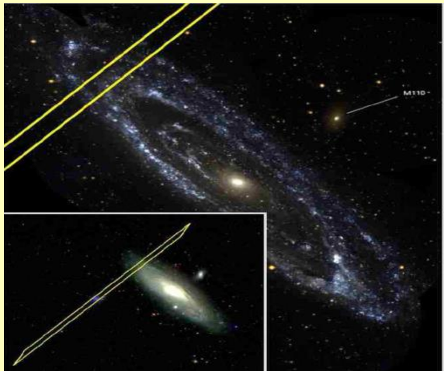

EXPECTED RATES FOR ADVANCED DETECTORS

2017-2020

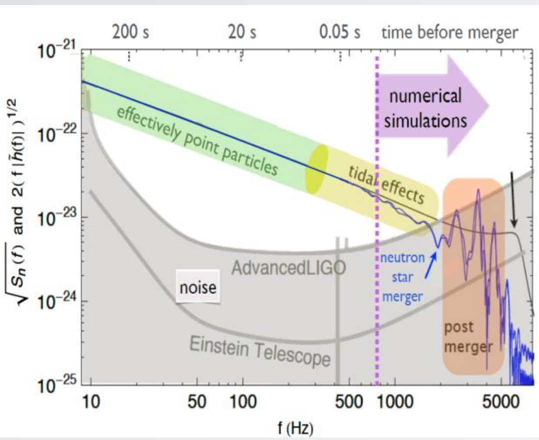

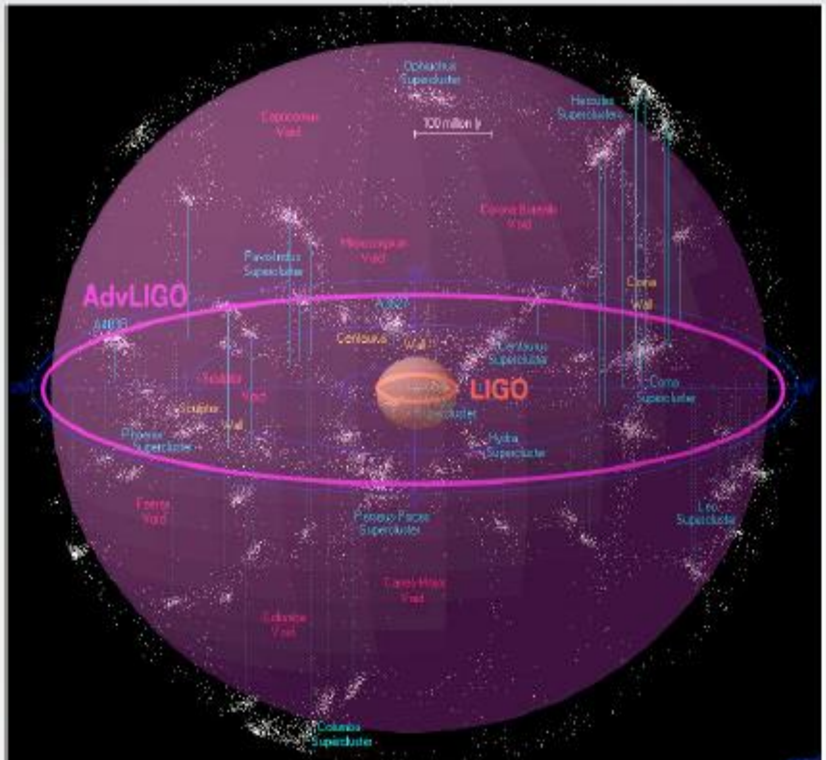

Network	Source	$\dot{N}_{low}$ (yr^{-1})	$\dot{N}_{re}$ (yr^{-1})	$\dot{N}_{high}$ (yr^{-1})
Initial	NS-NS	2×10^{-4}	0.02	0.2
	NS-BH	7×10^{-5}	0.0004	0.1
	BH-BH	2×10^{-4}	0.007	0.5
Advanced	NS-NS	0.4	40	400
	NS-BH	0.2	10	300
	BH-BH	0.4	20	1000

Future Einstein Telescope Project $\sim$ 2025: up to 10^4 CBC

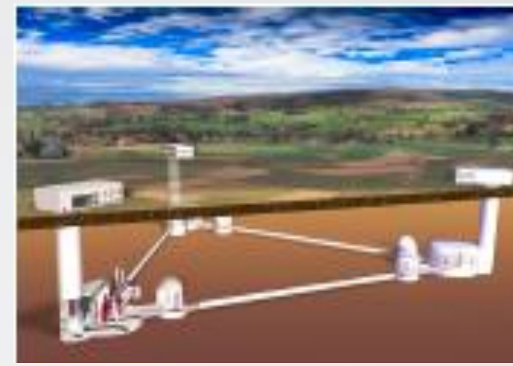

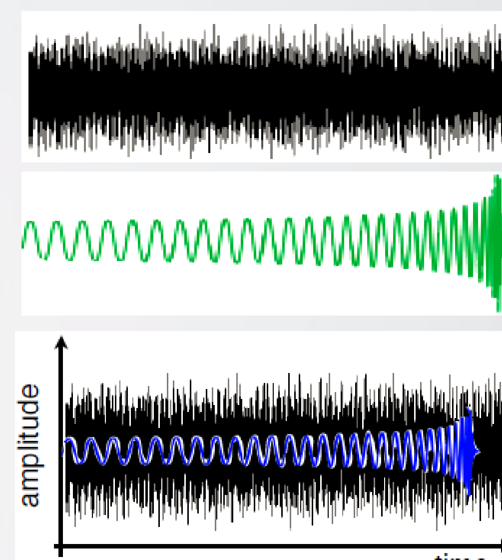

The Universe as seen in different wave lengths

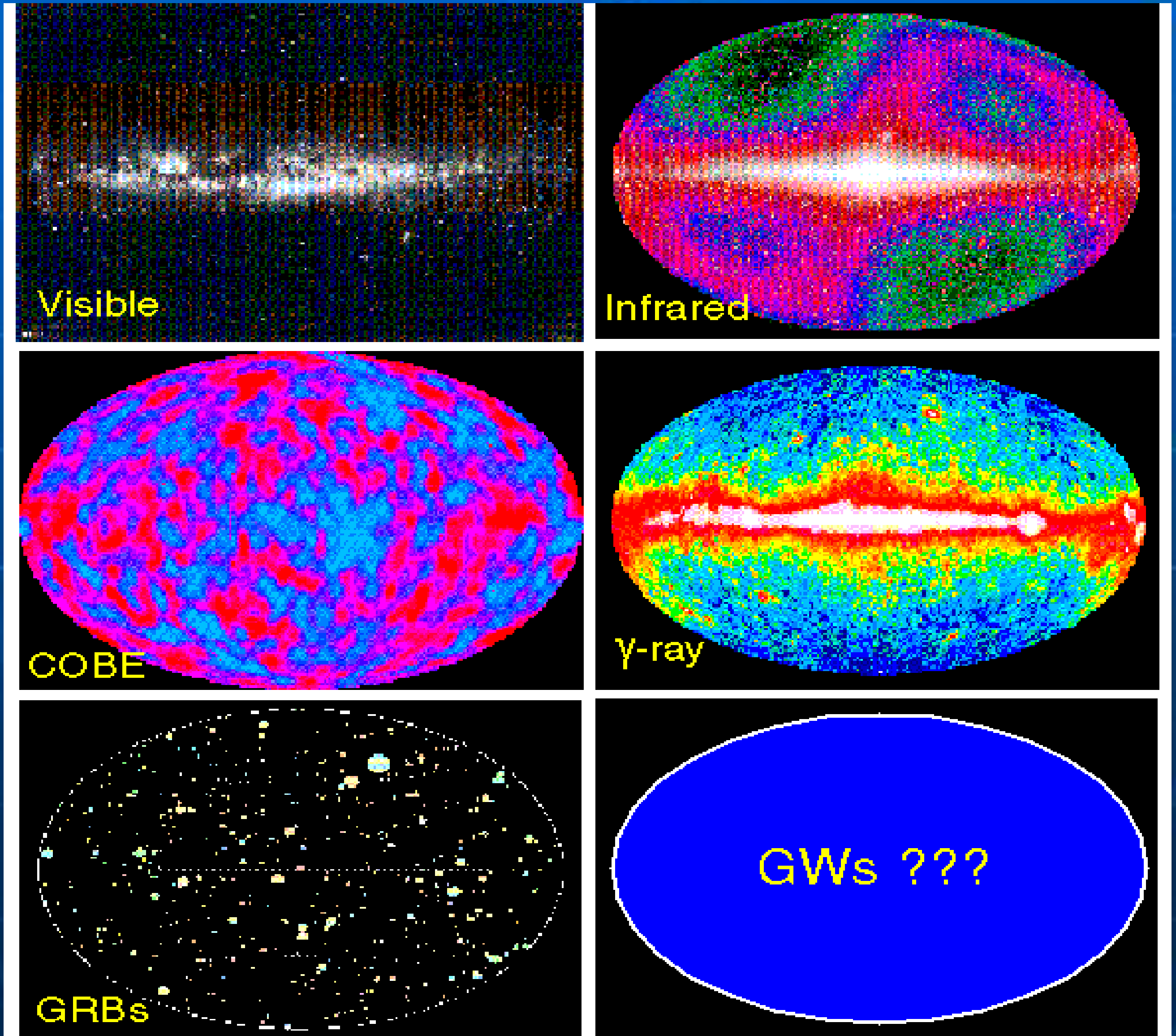

BICEP2, 2014
First step to Gravitational Astronomy

The Evolution of the Universe

t	$\rho^{1/4}$	T	Event
10^{-42} s	10^{18} GeV	~ 0	Inflation begins ? **BICEP2 (2014)**
$10^{-36\pm6}$ s	$10^{13\pm3}$ GeV	~ 0	Inflation ends, Cold Big Bang starts? **BICEP2 (2014)**
$10^{-18\pm6}$ s	$10^{6\pm3}$ GeV	$10^{6\pm3}$ GeV	Hot Big Bang begins ? **BICEP2 (2014)**
10^{-10} s	100 GeV	100 GeV	Electroweak phase transition ? **(LHC)**
10^{-4} s	100 MeV	100 MeV	Quark-hadron phase transition? **(LHC)**
10^{-2} s	10 MeV	10 MeV	γ, ν, $e^{\mp}$, n, p in thermal equilibrium
1 s	1 MeV	1 MeV	ν decoupling, $e^{\mp}$ annihilation
100 s	0.1 MeV	0.1 MeV	Nucleosynthesis
10^{4} yr	1 eV	1 eV	Matter-radiation equality
10^{5} yr	0.1 eV	0.1 eV	Atom formation, photon decoupling
$\sim$ 10^{9} yr	10^{-3} eV	10^{-4} eV	First bound structures forms
Now	3× 10^{-3} $h^{1/2}(\boldsymbol{\Omega}_0)^{1/4}$eV	**2.72548 ± 0.00057 K**	The present state of Universe

Wilkinson Microwave Anisotropy Probe (WMAP) 2003

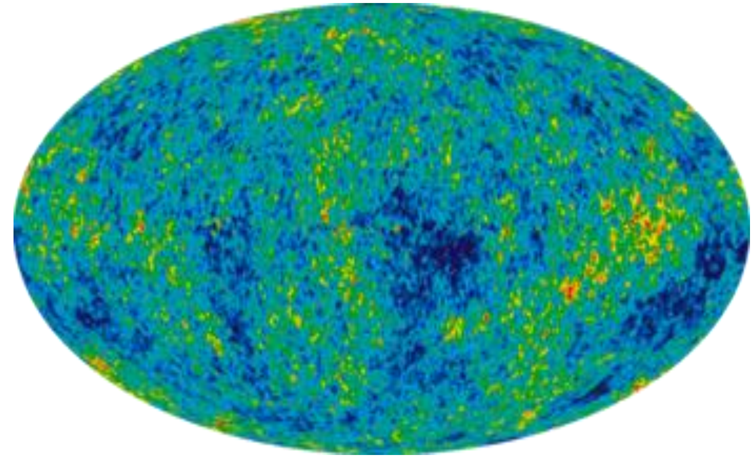

Best-fit cosmological parameters from WMAP five-year results[9]			
Parameter	Symbol	Best fit (WMAP only)	Best fit (WMAP + SNe + BAO)
Age of the universe (Ga)		13.69±0.13	13.72±0.12
Hubble's constant (km/Mpc·s)		$71.9^{+2.6}_{-2.7}$	70.5±1.3
Baryonic content		0.02273±0.00062	$0.02267^{+0.00058}_{-0.00059}$
Cold dark matter content		0.1099±0.0062	0.1131±0.0034
Dark energy content		0.742±0.030	0.726±0.015
Optical depth to reionization		0.087±0.017	0.084±0.016
Scalar spectral index		$0.963^{+0.014}_{-0.015}$	0.960±0.013
Running of spectral index		−0.037±0.028	−0.028±0.020
Fluctuation amplitude at $8h^{-1}$ Mpc		0.796±0.036	0.812±0.026
Total density of the universe		$1.099^{+0.100}_{-0.085}$	$1.0050^{+0.0060}_{-0.0061}$
Tensor-to-scalar ratio	r	< 0.43	< 0.22

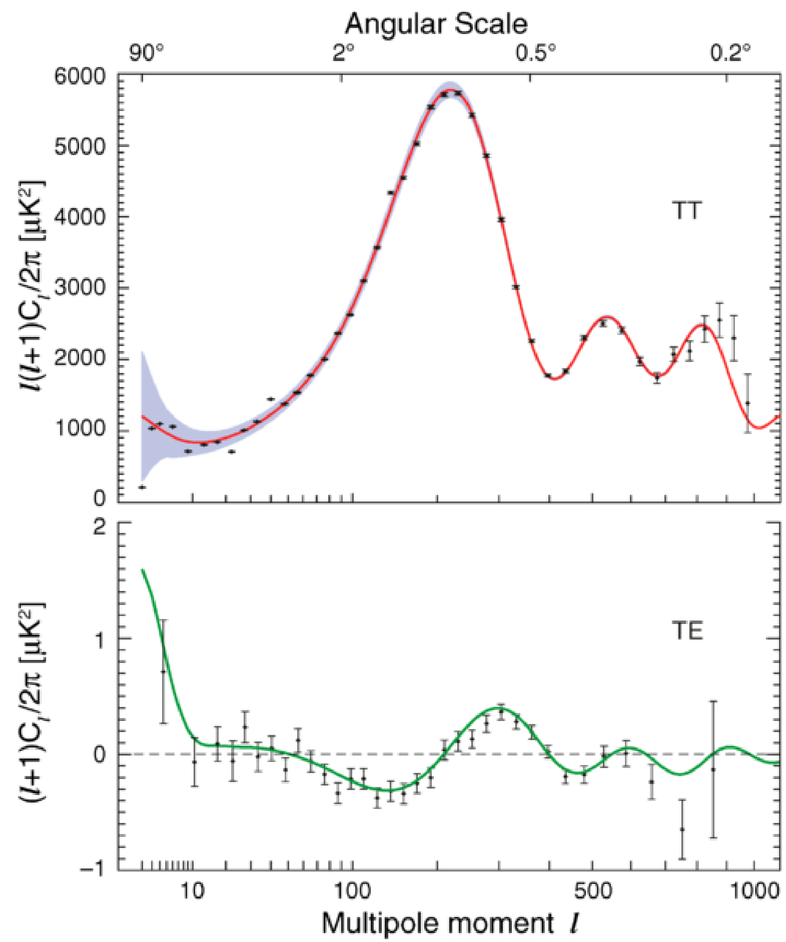

Published Results of Planck Mission

Data acquired in the period
12 August 2009 to 27 November 2010
(15.5 months)

On **22 March 2013** the Planck collaboration published at once **29** new articles, from

http://arxiv.org/abs/1303.5062v1
to
http://arxiv.org/abs/1303.5090v1

which

change essentially our understanding of the Universe

22 LFI radio receivers and
52 HFI bolometric detectors
in the range 25 – 1000 GHz

Plank 2013 CMB precise picture:

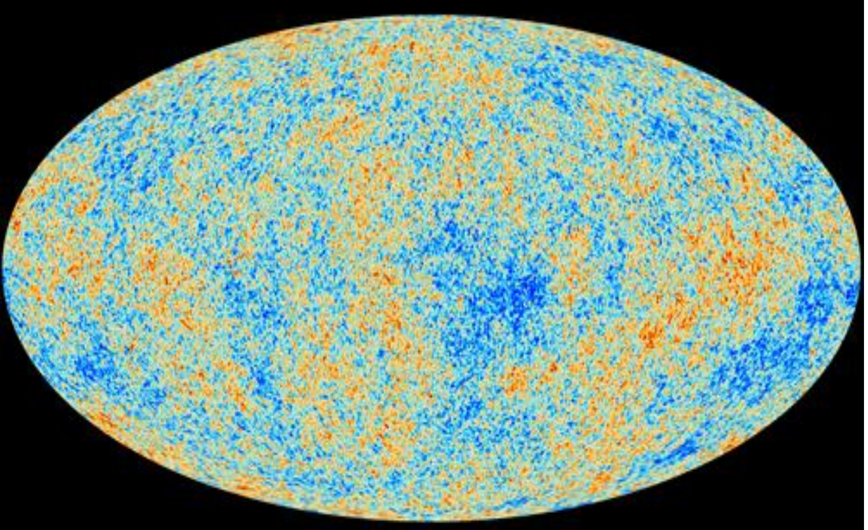

Last scattering surface
(380,000 years after the Beginning)

Precise measurement of seven acoustic peaks, that are well fit ***by a simple six-parameter ΛCDM theoretical model.***

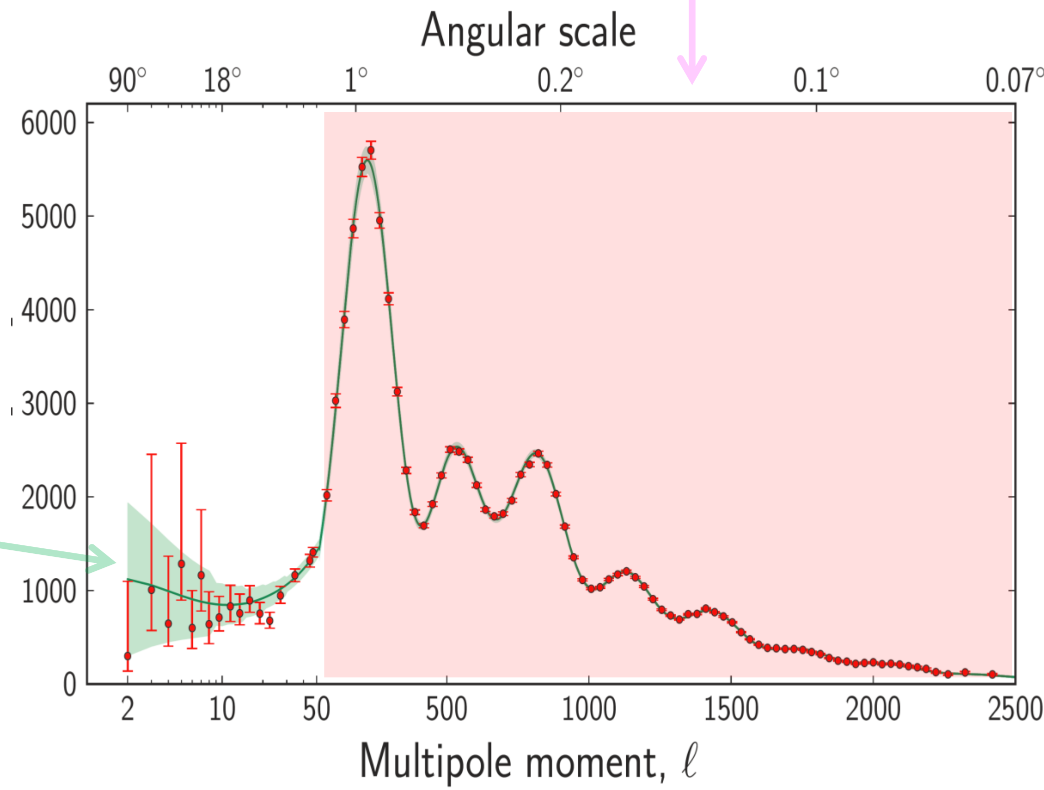

The unusual shape of the spectrum in the multipole range 20 < l < 60 is a real feature of the primordial CMB anisotropies.

Plank 2013 Cosmological Parameters:

lower Hubble constant $H_0 = (67 \pm 1.2)\ \mathrm{km\,s^{-1}\,Mpc^{-1}}$

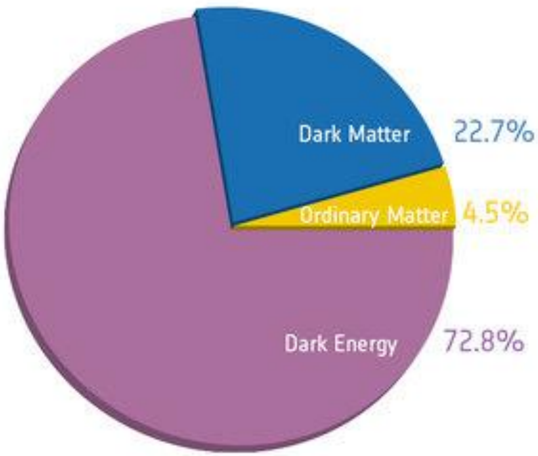

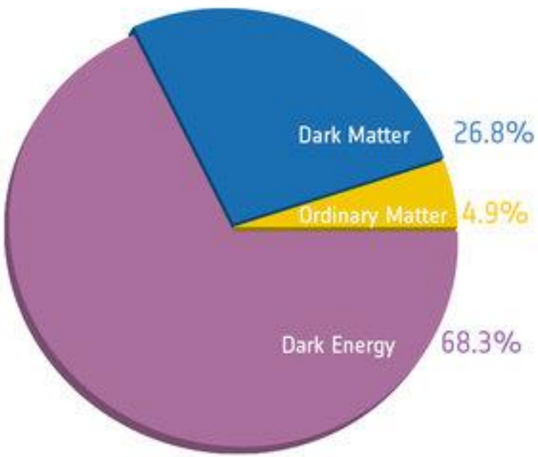

higher Ω_{CDM} (by ~18 %)

higher $\Omega_{baryons}$ (by ~9 %)

lower Ω_Λ (by ~6 %)

$\Omega_K = -0.0096^{+0.010}_{-0.0082}$ (68 % CL)

$\Omega_b \approx 0.05,\ \Omega_{cdm} \approx 0.23,\ \Omega_\Lambda \approx 0.72$

Before Planck

$$h = 0.704 \pm 0.025$$

$$\Omega_c h^2 = 0.112 \pm 0.006$$

$$\Omega_b h^2 = 0.0225 \pm 0.0006$$

$$\Omega_\Lambda = 0.73 \pm 0.03$$

$$w = -0.91^{+0.16}_{-0.20}\,(\mathrm{stat.})^{+0.07}_{-0.14}\,(\mathrm{sys.})$$

After Planck

$\Omega_m = 0.315^{+0.016}_{-0.018}$

$\Omega_c h^2 = 0.1199 \pm 0.0027$

$\Omega_b h^2 = 0.02205 \pm 0.00028$

$w = -1.13^{+0.13}_{-0.10}$

$\Omega_\Lambda = 0.67^{+0.027}_{-0.023}$ (68 % CL)

Planck 2013 picture of the Universe:

Present radius of the visible Universe $1/\sqrt{\Lambda} \approx$ 8.88×10^{22} km ➡ 9.633×10^{22} km

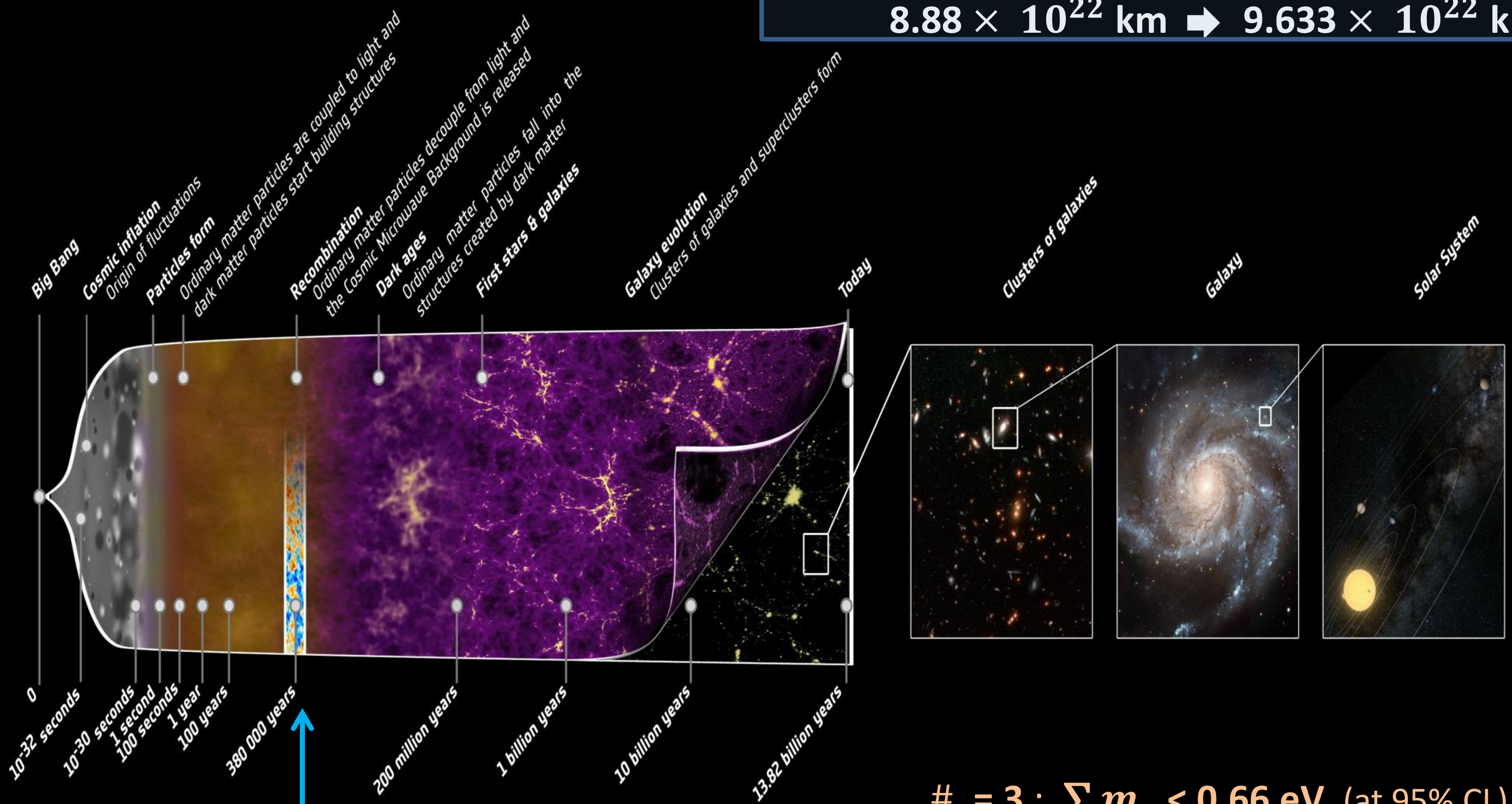

$\#_\nu = 3$; $\sum m_\nu < 0.66$ eV (at 95% CL)

Any variation in the fine-structure constant from Recombination to the present day is $\leq 0.4\%$.

Age/Gyr Old: 13.75 +/- 0.1
New: 13.817 ± 0.048

Some theoretical explanations:

THE PRIMORDIAL DENSITY PERTURBATION,
DAVID H . LYTH, ANDREW R . LIDDLE,
Cambridge University Press, 2009

GR:

$$R_{\mu\nu} - \frac{1}{2} g_{\mu\nu} R = 8\pi G T_{\mu\nu}$$

FRW Universe:

$$ds^2 = -dt^2 + a^2(t)\left[\frac{dx^2}{1-Kx^2} + x^2\left(d\theta^2 + \sin^2\theta\, d\phi^2\right)\right]$$

Hubble parameter H(t) : $H \equiv \dot{a}/a$, H_0 $-$ *present value*

The number N of e-folds of expansion $N \equiv \ln \frac{a_2}{a_1}$

Continuity equation:

$$a\frac{d\rho}{da} = -3(\rho + P)$$

Friedmann equation:

$$H^2 = \frac{\rho}{3M_{\rm Pl}^2} - \frac{K}{a^2}$$

Acereleration equation: $\dot{H} + H^2 = -\frac{\rho + 3P}{6M_{\rm Pl}^2}$

$$\Omega(t) = \frac{\rho(t)}{\rho_{\rm crit}(t)}$$

$\rho_{\rm crit}$ is defined as $3M_{\rm Pl}^2 H^2(t)$ ⇒

$$\Omega - 1 \equiv \frac{K}{a^2 H^2} \equiv \frac{K}{\dot{a}^2}$$

$\Omega_K = -0.0096^{+0.010}_{-0.0082}$ (68 % CL) ⇒ $\Omega = 1$

$$ds^2 = -dt^2 + a^2(t)\left(dx^2 + dy^2 + dz^2\right)$$

Primordial density perturbations:

$$\rho = \rho_\nu + \rho_\gamma + \rho_B + \rho_c \quad \Rightarrow \quad \rho_a(R,\mathbf{x},t) = \rho_a(t) + \delta\rho_a(R,\mathbf{x},t)$$

$$|\delta\rho_a(R,\mathbf{x},t)/\rho_a(t)| \ll 1$$

For R - a radius of cosmological scale
$\rho_a(\mathbf{x},t)$ is replaced by a smoothed one $\rho_a(R,\mathbf{x},t)$

Assumptions: 1. **adiabatic condition** for the quantity ρ_a

2. For Fourier components of $\delta\rho_\mathbf{k}$: No other relations except $\delta\rho^*_\mathbf{k} = \delta\rho_{-\mathbf{k}}$

3. $\delta\rho$ is **gaussian**

4. $\delta\rho(R,\mathbf{x})$ is almost independent of R – scale invariant.

5. $\mathcal{P}_\zeta^{1/2}$ - related with **rms value** of $\delta\rho$ is fundamental quantity for cosmology.

6. Observationally $\delta\rho$ is about 5×10^{-5} and shows

Small deviations from the scale invariance, measured by **the spectral index** **n** .

Perturbations of metric:

$$g_{ij} = a^2(\mathbf{x},t)\gamma_{ij}(\mathbf{x})$$

$$a(\mathbf{x},t) \equiv a(t)e^{\zeta(\mathbf{x},t)}, \qquad \gamma_{ij}(\mathbf{x}) \equiv \left(Ie^{h}\right)_{ij}$$

One can choose local coordinates: $\gamma_{ij} = \delta_{ij}$.

Gauge invariant quantities

$$\zeta(\mathbf{x},t) = \delta N(\mathbf{x},t)$$

$$\tilde{t} = t + \delta t(\mathbf{x},t) \qquad \psi = \zeta - H\delta t$$

← **Curvature perturbations**

$$\delta\rho(\mathbf{x},t) = -\dot{\rho}(t)\delta t(\mathbf{x},t)$$

$$\zeta = -H\frac{\delta\rho}{\dot{\rho}} = \frac{1}{3}\frac{\delta\rho}{\rho + P}$$

For multicomponent fluid: $\zeta_{\mathrm{a}} \equiv -\dfrac{H\delta\rho_{\mathrm{a}}}{\dot{\rho}_{\mathrm{a}}} = \dfrac{1}{3}\dfrac{\delta\rho_{\mathrm{a}}}{\rho_{\mathrm{a}} + P_{\mathrm{a}}}$

Random fields g(x):

Two point correlator: $\langle g(\mathbf{x}) g(\mathbf{x}')\rangle \equiv \sum_n \mathbf{P}_n g_n(\mathbf{x}) g_n(\mathbf{x}')$

$g_n(\mathbf{x})$
- with probability
$\mathbf{P}_n$

Fourier transform: $g(\mathbf{x}) = \frac{1}{L^3}\sum_n g_n e^{i\mathbf{k}_n\cdot\mathbf{x}}, \qquad g_n = \int g(\mathbf{x}) e^{-i\mathbf{k}_n\cdot\mathbf{x}} d^3x$

Gaussian perturbations in momentum space:

$$\mathbf{P}(g) = \frac{1}{\sqrt{2\pi}\sigma}\exp\left(-\frac{g^2}{2\sigma_g^2}\right)$$

$\langle g_n g_m^*\rangle = \delta_{nm} P_{g_n} \qquad P_{g_n} \quad P_g(k) g_n|^2\rangle \qquad \langle g_n g_m\rangle = \delta_{n,-m} P_{g_n}$

The spectrum $P_g(k)$ **is defined In continuum limit as:** $L^{-3} P_{g_n} \rightarrow P_g(k)$

The convenient quantity
$\mathcal{P}_g \equiv (k^3/2\pi^2) P_g$
Is often called SPECTRUM

The spectral index:
(characterizes the scale dependence)

$$n - 1 \equiv \frac{d\ln \mathcal{P}_\zeta(k)}{d\ln k}$$

If $n(k)$ is constant, $\mathcal{P}_\zeta(k) \propto k^{n-1}$
If n depends on k one says that
the spectral index is **running**. $\quad n' \equiv dn/d\ln k$

CMB spectrum:

Brightness Function:

$$\Theta(\eta, \mathbf{x}, \mathbf{n}) \equiv \frac{\delta T(\eta, \mathbf{x}, \mathbf{n})}{T(\eta)}$$

$$\Theta(\eta, \mathbf{x}, \mathbf{n}) = \sum_{\ell m} (-1)^{\ell} \Theta_{\ell m}(\eta, \mathbf{x}) Y_{\ell m}(\mathbf{n}) = \sum_{\ell m} \Theta_{\ell m}(\eta, \mathbf{x}) Y_{\ell m}(\mathbf{e})$$

Intrinsic anisotropy:

$$a_{\ell m} \equiv \Theta_{\ell m}(\eta_0, \mathbf{x}_0)$$

$$\langle a_{\ell m} a^*_{\ell' m'} \rangle = \delta_{\ell \ell'} \delta_{m m'} C_\ell$$

The spectrum of the CMB anisotropy:

$$C(\theta) \equiv \langle \Theta(\mathbf{e}_1) \Theta(\mathbf{e}_2) \rangle = \sum_{\ell} \frac{2\ell + 1}{4\pi} C_\ell P_\ell(\cos\theta)$$

$$C_\ell = \langle |a_{\ell m}|^2 \rangle$$

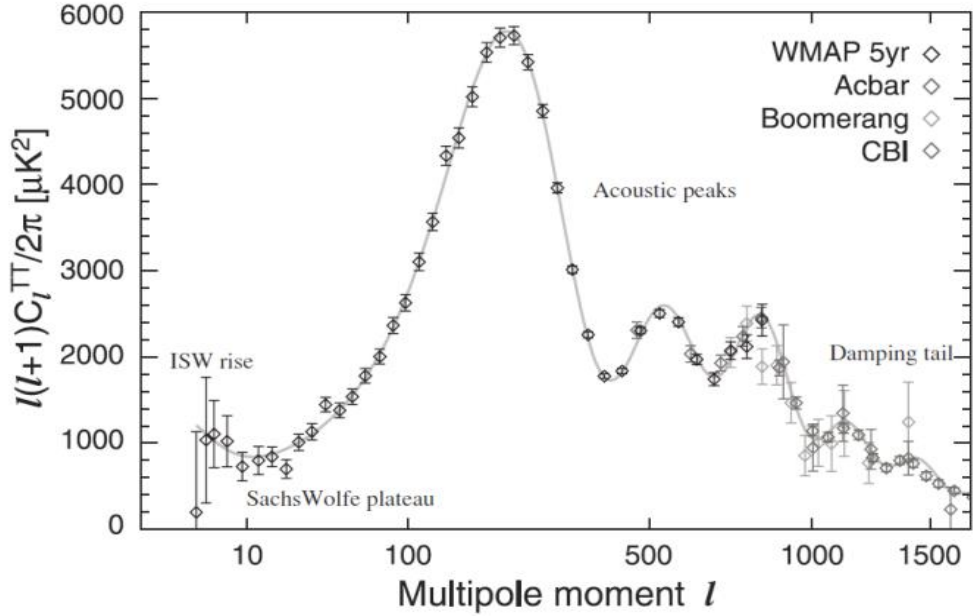

Polarized EM radiation in CMB:

$$\mathbf{E}(t) = \mathrm{Re}\left[\mathbf{E}e^{i\omega t}\right] = \frac{1}{2}\left(\mathbf{E}e^{i\omega t} + \mathbf{E}^* e^{-i\omega t}\right)$$

in a plane with azimuthal angle ϕ $\quad E_\phi = E_x \cos\phi + E_y \sin\phi$

The intensity measured By detector is:

$$\frac{dI}{d\omega} = \overline{|E_\phi^2|} = I + Q\cos 2\phi + U \sin 2\phi$$

$$I \equiv \overline{|E_x|^2} + \overline{|E_y|^2},$$
$$Q \equiv \overline{|E_x|^2} - \overline{|E_y|^2},$$
$$U \equiv 2\,\mathrm{Re}\,\overline{E_x^* E_y},$$

Stokes parameters

For $Q_\pm \equiv Q \pm iU$

$$Q_\pm(\mathbf{e}) = \sum_{\ell=2}^{\infty}\sum_{m=-\ell}^{\ell}(-1)^\ell Q_{\ell m}^{\pm} Y_{\ell m}^{\mp}(\mathbf{n}) = \sum_{\ell=2}^{\infty}\sum_{m=-\ell}^{\ell} Q_{\ell m}^{\pm} Y_{\ell m}^{\pm}(\mathbf{e})$$

Polarization multipoles $E_{\ell m}$ and $B_{\ell m}$ are defined by

$$Q_{\ell m}^{\pm} = E_{\ell m} \pm i B_{\ell m}.$$

$$\langle a_{\ell m}^* a_{\ell' m'}\rangle = C_\ell\, \delta_{\ell\ell'}\delta_{mm'}, \qquad \langle a_{\ell m}^* E_{\ell' m'}\rangle = C_\ell^{TE}\, \delta_{\ell\ell'}\delta_{mm'},$$

$$\langle E_{\ell m}^* E_{\ell' m'}\rangle = C_\ell^{EE}\, \delta_{\ell\ell'}\delta_{mm'}, \qquad \langle B_{\ell m}^* B_{\ell' m'}\rangle = C_\ell^{BB}\, \delta_{\ell\ell'}\delta_{mm'},$$

Tensor perturbations:

$$ds^2 = a^2(\eta)\left[-d\eta^2 + (\delta_{ij} + 2h_{ij})\,dx^i dx^j\right]$$

h_{ij} is traceless and transverse

Einstein Eqs. give

$$\ddot{h}_{ij} + 2aH\dot{h}_{ij} + k^2 h_{ij} = 8\pi G \Sigma^{\mathrm{T}}_{ij}$$

$h_{+,\times}(\mathbf{k},\eta)$

Σ^{T}_{ij} is the traceless and transverse part of the anisotropic stress

The spectrum $\mathcal{P}_h$ is defined by:

$$4\langle h_+(\mathbf{k}))h_+(\mathbf{k}')\rangle = 4\langle h_\times(\mathbf{k})h_\times(\mathbf{k}')\rangle = (2\pi)^3\frac{2\pi^2}{k^3}\mathcal{P}_h(k)\delta^3(\mathbf{k}-\mathbf{k}')$$

The spectrum $\mathcal{P}_\zeta$:

$$\ell(\ell+1)C_\ell = \frac{2\pi}{25}\mathcal{P}_\zeta(\ell/\eta_0)$$

The tensor fraction is defined by:

$$r \equiv \frac{\mathcal{P}_h}{\mathcal{P}_\zeta}$$

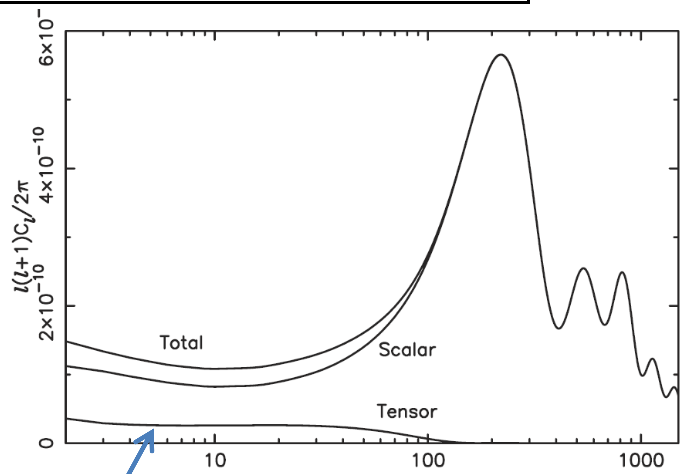

For $\ell \ll 100$ $\quad \ell(\ell+1)C_\ell = \frac{\pi}{9}\left(1 + \frac{48\pi^2}{385}\right)\mathcal{P}_h c_\ell$

$c_2 = 1.118,\ c_3 = 0.878,$
$c_4 = 0.819$ with $c_\infty = 1$

Inflation with one scalar field in EF:

$$\mathcal{L} = -\frac{1}{2}\partial^\mu\phi\partial_\mu\phi - V(\phi)$$

More general: $\mathcal{L} = -\frac{1}{2}G(\phi)\partial^\mu\phi\,\partial_\mu\phi - V(\phi)$

$$-\Box\phi + V'(\phi) = 0$$

$\boldsymbol{\phi}$(t) ⇒ $\ddot{\phi}_n + 3H\dot{\phi}_n + \frac{\partial V}{\partial \phi_n} = 0$ -- FRW space-time

$\rho = \frac{1}{2}\dot{\phi}^2 + V(\phi)$, $P = \frac{1}{2}\dot{\phi}^2 - V(\phi)$

$V(\phi) = \frac{1}{2}m^2\phi^2 + \frac{1}{4}\lambda\phi^4 + \lambda_6\frac{\phi^6}{\Lambda^2} + \lambda_8\frac{\phi^8}{\Lambda^4} + \ldots$

$3M_{\rm Pl}^2H^2 = V(\phi) + \frac{1}{2}\dot{\phi}^2$

Quantization:

$$\begin{aligned}\hat{\phi}(\mathbf{x},t) &= L^{-3}\sum_{\mathbf{k}}\left[\phi_k(t)\hat{a}_{\mathbf{k}}e^{i\mathbf{k}\cdot\mathbf{x}} + \phi_k^*(t)\hat{a}_{\mathbf{k}}^\dagger e^{-i\mathbf{k}\cdot\mathbf{x}}\right] \\ &= L^{-3}\sum_{\mathbf{k}}\left[\phi_k(t)a_{\mathbf{k}} + \phi_k^*(t)a_{-\mathbf{k}}^\dagger\right]e^{i\mathbf{k}\cdot\mathbf{x}}.\end{aligned}$$

$$L^{-3}[\hat{a}_{\mathbf{k}}, \hat{a}_{\mathbf{k}'}^\dagger] = \delta_{\mathbf{k}\mathbf{k}'}$$

INFLATION $\Longleftrightarrow$ $\ddot{a} > 0$ $\Longleftrightarrow$ $\rho + 3P < 0$

The slow-roll paradigm :

$|\ddot{\phi}| \ll 3H|\dot{\phi}|$ ⇒ $3H\dot{\phi} \simeq -V'(\phi)$ **or** $\epsilon(\phi) \ll 1$ where $\epsilon \equiv \frac{M_{\rm Pl}^2}{2}\left(\frac{V'}{V}\right)^2$

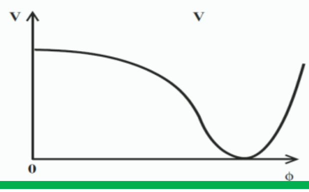

and $|\eta(\phi)| \ll 1$ where $\eta \equiv M_{\rm Pl}^2\frac{V''}{V} \simeq \frac{V''}{3H^2}$

Background Imaging of Cosmic Extragalactic Polarization (BICEP)

A SCIENTIFIC BREAKTHROUGH LETS US SEE TO THE BEGINNING OF TIME

Download Press Conference at the Harvard-Smithsonian Center for Astrophysics:

http://www.cfa.harvard.edu/pao/Bicep2_press_con.mov

John Covach, Chao-Lin Kuo, Jamie Bock, Clem Pryke, Marc Kamionkowsky

Popular movie:

http://bcove.me/2z2qriut

Detection of B-mode Polarization at Degree Scales using BICEP2:

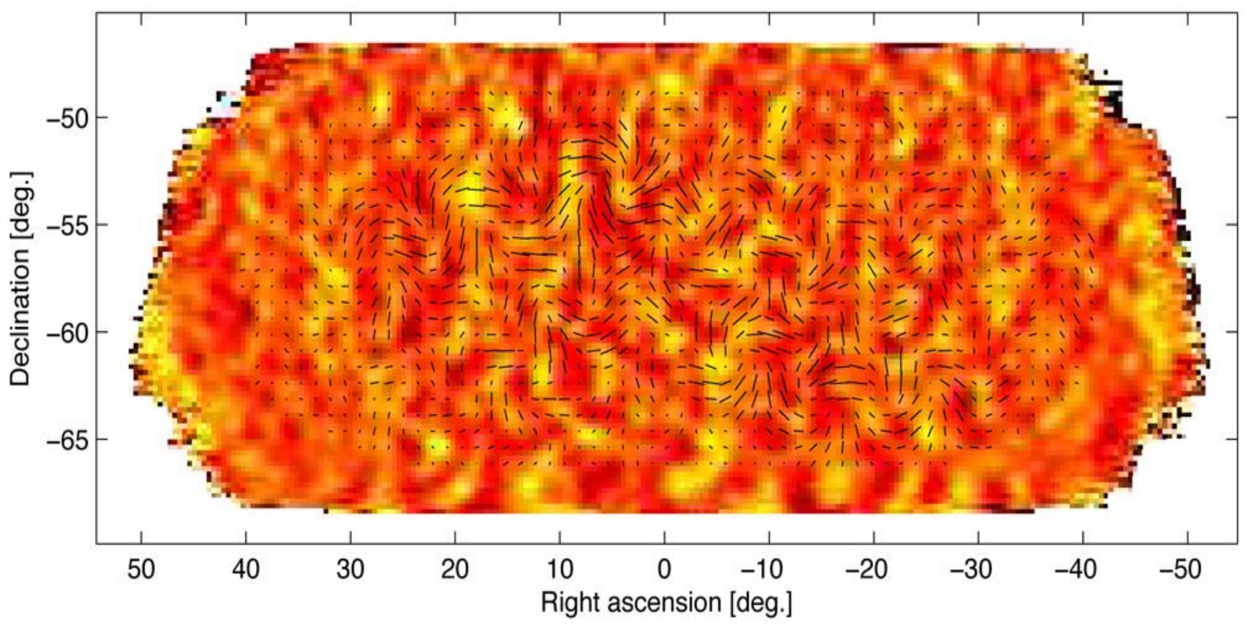

Only gravitational waves can produce B-mode Polarization !

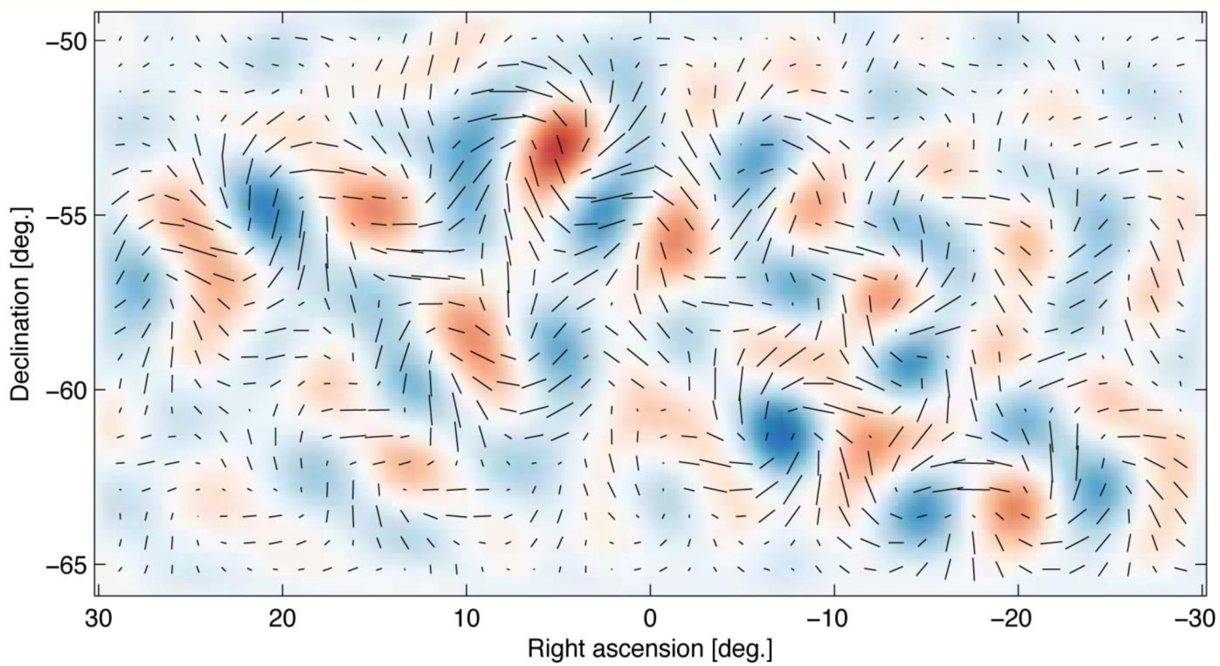

BICEP 2

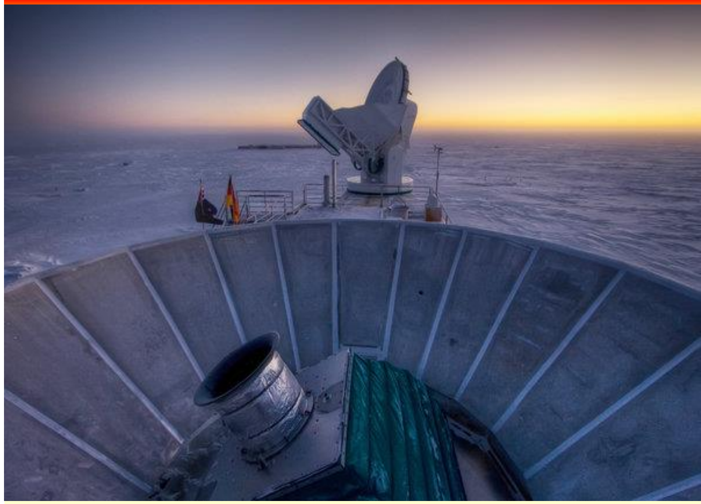

arXiv:1403.3985v1 [astro-ph.CO] 17 Mar 2014

BICEP2 I: DETECTION OF *B*-mode POLARIZATION AT DEGREE ANGULAR SCALES

BICEP2 COLLABORATION - P. A. R. ADE[1], R. W. AIKIN[2], D. BARKATS[3], S. J. BENTON[4], C. A. BISCHOFF[5], J. J. BOCK[2,6], J. A. BREVIK[2], I. BUDER[5], E. BULLOCK[7], C. D. DOWELL[6], L. DUBAND[8], J. P. FILIPPINI[2], S. FLIESCHER[9], S. R. GOLWALA[2], M. HALPERN[10], M. HASSELFIELD[10], S. R. HILDEBRANDT[2,6], G. C. HILTON[11], V. V. HRISTOV[2], K. D. IRWIN[12,13,11], K. S. KARKARE[5], J. P. KAUFMAN[14], B. G. KEATING[14], S. A. KERNASOVSKIY[12], J. M. KOVAC[5,16], C. L. KUO[12,13], E. M. LEITCH[15], M. LUEKER[2], P. MASON[2], C. B. NETTERFIELD[4], H. T. NGUYEN[6], R. O'BRIENT[6], R. W. OGBURN IV[12,13], A. ORLANDO[14], C. PRYKE[9,7,16], C. D. REINTSEMA[11], S. RICHTER[5], R. SCHWARZ[9], C. D. SHEEHY[9,15], Z. K. STANISZEWSKI[2,6], R. V. SUDIWALA[1], G. P. TEPLY[2], J. E. TOLAN[12], A. D. TURNER[6], A. G. VIEREGG[5,15], C. L. WONG[5], AND K. W. YOON[12,13]

to be submitted to a journal TBD

ABSTRACT

We report results from the BICEP2 experiment, a Cosmic Microwave Background (CMB) polarimeter specifically designed to search for the signal of inflationary gravitational waves in the *B*-mode power spectrum around $\ell \sim 80$. The telescope comprised a 26 cm aperture all-cold refracting optical system equipped with a focal plane of 512 antenna coupled transition edge sensor (TES) 150 GHz bolometers each with temperature sensitivity of $\approx 300\ \mu\mathrm{K}_{\mathrm{CMB}}\sqrt{s}$. BICEP2 observed from the South Pole for three seasons from 2010 to 2012. A low-foreground region of sky with an effective area of 380 square degrees was observed to a depth of 87 nK-degrees in Stokes Q and U. In this paper we describe the observations, data reduction, maps, simulations and results. We find an excess of *B*-mode power over the base lensed-ΛCDM expectation in the range $30 < \ell < 150$, inconsistent with the null hypothesis at a significance of $> 5\sigma$. Through jackknife tests and simulations based on detailed calibration measurements we show that systematic contamination is much smaller than the observed excess. We also estimate potential foreground signals and find that available models predict these to be considerably smaller than the observed signal. These foreground models possess no significant cross-correlation with our maps. Additionally, cross-correlating BICEP2 against 100 GHz maps from the BICEP1 experiment, the excess signal is confirmed with 3σ significance and its spectral index is found to be consistent with that of the CMB, disfavoring synchrotron or dust at 2.3σ and 2.2σ, respectively. The observed *B*-mode power spectrum is well-fit by a lensed-ΛCDM + tensor theoretical model with tensor/scalar ratio $r = 0.20^{+0.07}_{-0.05}$, with $r = 0$ disfavored at 7.0σ. Subtracting the best available estimate for foreground dust modifies the likelihood slightly so that $r = 0$ is disfavored at 5.9σ.

Subject headings: cosmic background radiation — cosmology: observations — gravitational waves — inflation — polarization

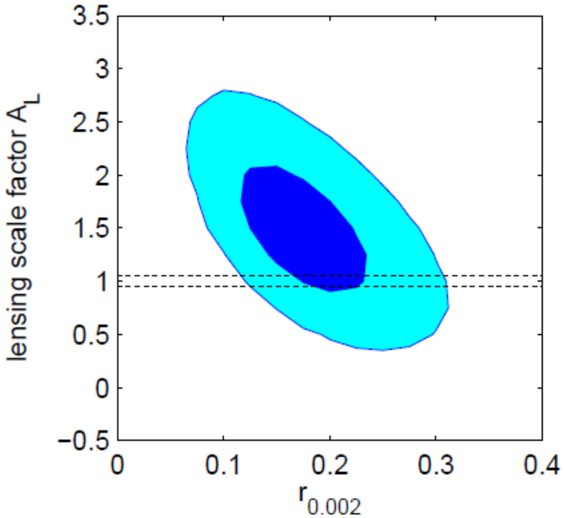

FIG. 12.— Joint constraints on the tensor-to-scalar ratio r and the lensing scale factor A_L using the BICEP2 *BB* bandpowers 1–5. One and two σ contours are shown. The horizontal dotted lines show the 1σ constraint from Planck Collaboration XVI (2013). The BICEP2 data are compatible with the expected amplitude of the lensing *B*-mode which is detected at 2.7σ.

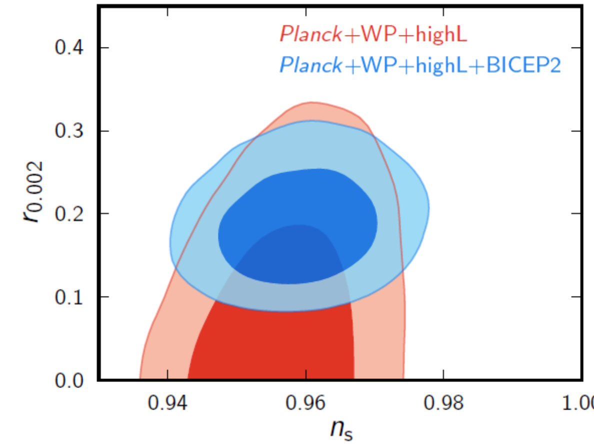

FIG. 13.— Indirect constraints on r from CMB temperature spectrum measurements relax in the context of various model extensions. Shown here is one example, following Planck Collaboration XVI (2013) Figure 23, where tensors and running of the scalar spectral index are added to the base ΛCDM model. The contours show the resulting 68% and 95% confidence regions

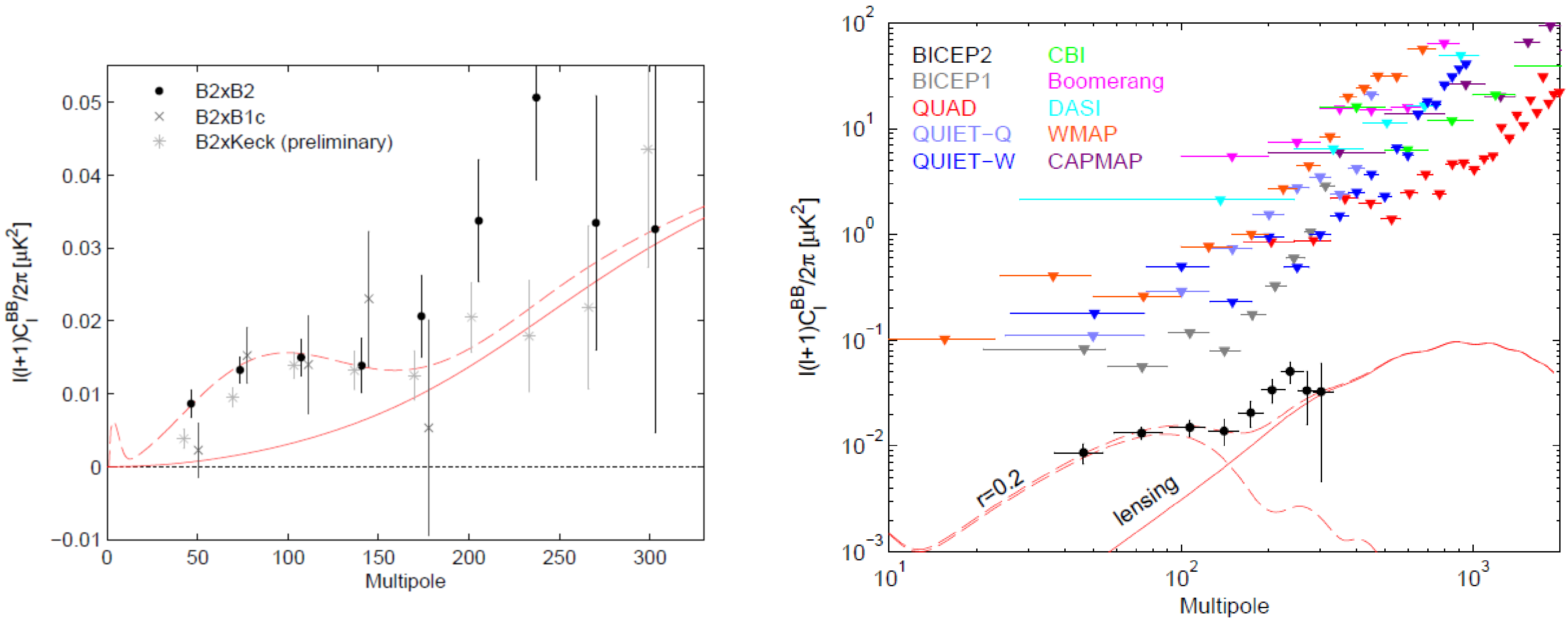

Basic results:

1. The simplest and most economical remaining interpretation of the *B*-mode signal which we have detected is that it is due to tensor modes — the IGW template is an excellent fit to the observed excess. We therefore proceed to set a constraint on the tensor-to-scalar ratio and find $r = 0.20^{+0.07}_{-0.05}$ with $r = 0$ ruled out at a significance of 7.0σ.

2. Subtracting the various dust models and re-deriving the r constraint still results in high significance of detection. For the model which is perhaps the most likely to be close to reality (DDM2 cross) the maximum likelihood value shifts to $r = 0.16^{+0.06}_{-0.05}$ with $r = 0$ disfavored at 5.9σ. These high values of r are in apparent tension with previous indirect limits based on temperature measurements and we have discussed some possible resolutions including modifications of the initial scalar perturbation spectrum such as running. However we emphasize that we do not claim to know what the resolution is.

arXiv:1403.4302v2 3 Apr 2014 BICEP2 II: EXPERIMENT AND THREE-YEAR DATA SET

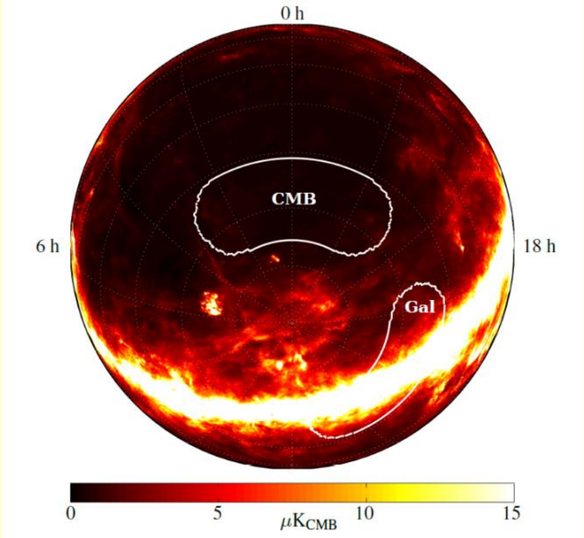

The full data set reached Stokes Q and U map depths of 87.2 nK in square-degree pixels (5:2 K arcmin) over an effective area of 383.7 square degrees within a 1000 square degree field.

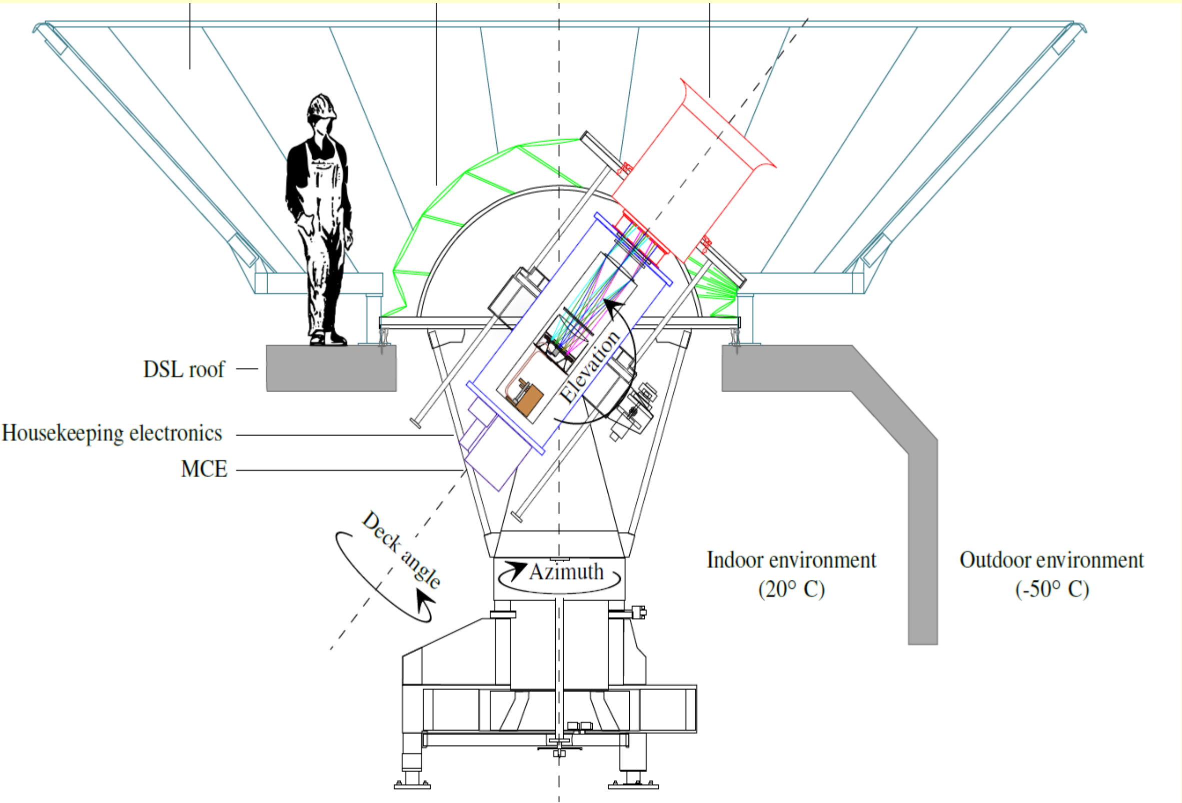

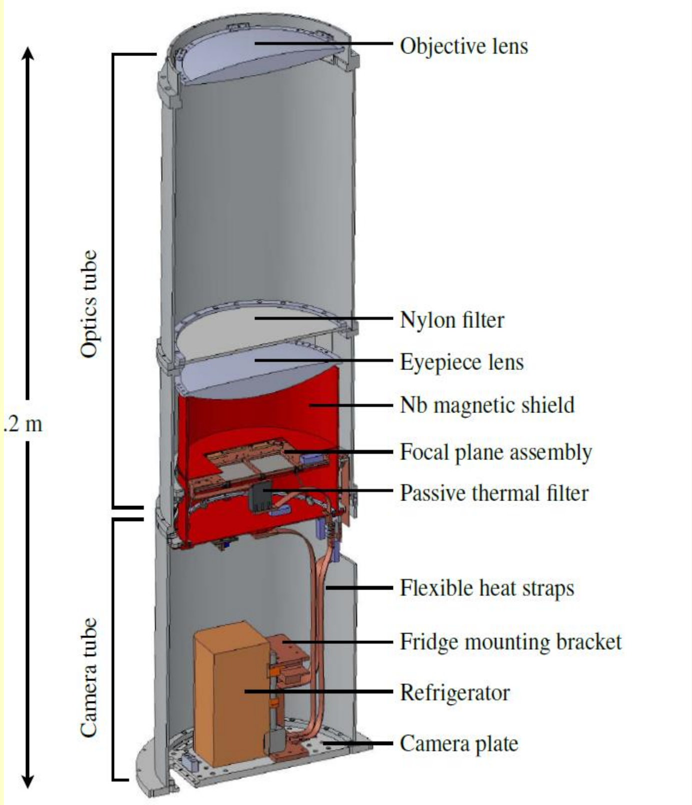

Ruling out the power-law form of the scalar primordial spectrum

arXiv:1403.7786 30 Mar 2014 *D.K. Hazra, A. Shafieloo, G.F. Smoot, A.A. Starobinsky*

Combining Planck CMB temperature and BICEP2 B-mode polarization data we show qualitatively that, assuming inflationary consistency relation, the power-law form of the scalar primordial spectrum is ruled out at more than 3σ CL.

$$P_S^{\mathrm{Tanh}}(k) = P_S^{\mathrm{Plaw}}(k) \times \left[1 + \alpha \tanh\left[\frac{k - k_b}{\Delta}\right]\right] \quad \& \quad \text{consistency relation } r = -8n_T$$

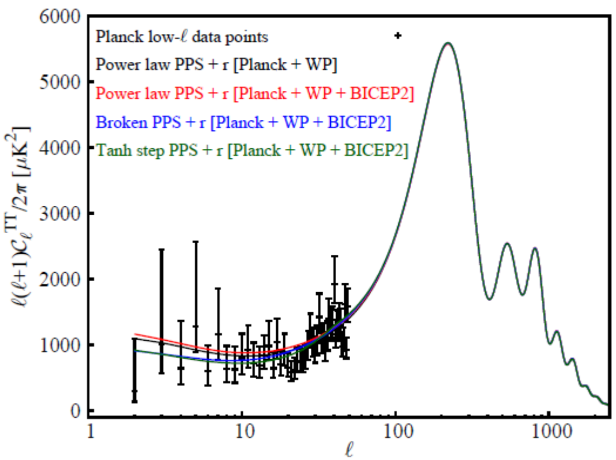

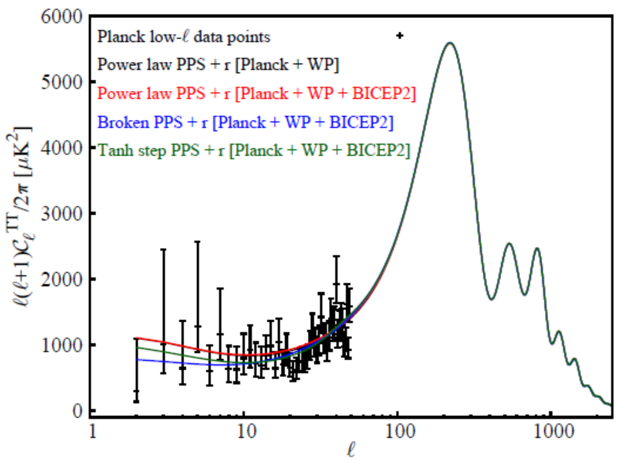

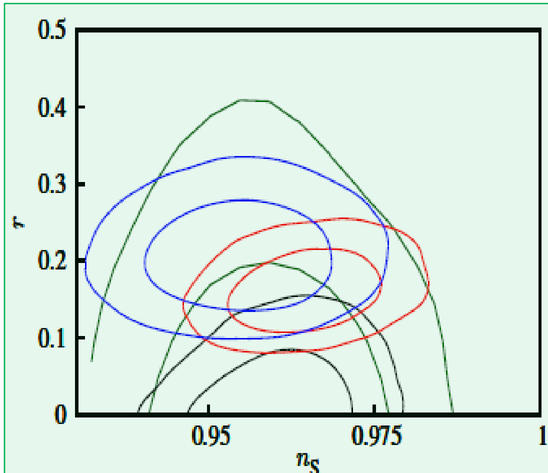

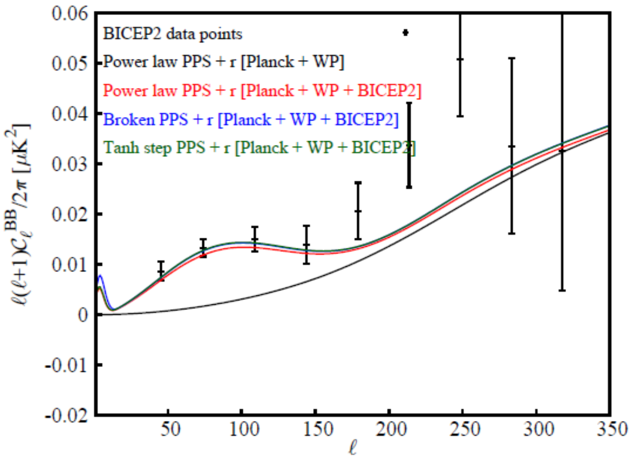

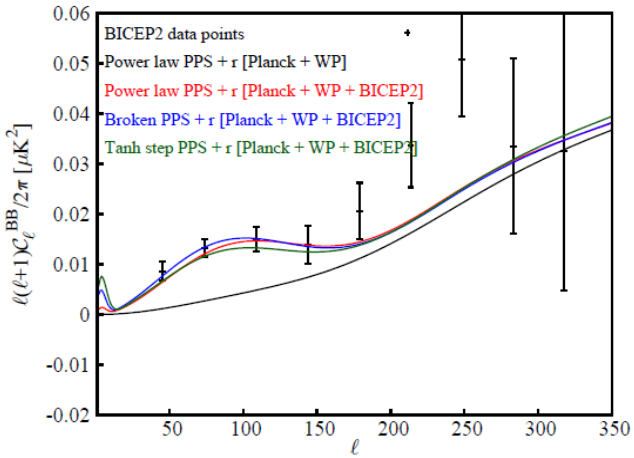

The broken Tanh power spectrum can address both the data from Planck and BICEP2 and can solve the inconsistencies within.

The Tanh step form of the PPS, can fit properly both Planck and BICEP2 data simultaneously.

Comparison of the Tanh step scalar PPS with power law spectra				
Tanh Model	Planck + WP		Planck + WP + BICEP2	
	$n_T = -r/8$	Variable n_T	$n_T = -r/8$	Variable n_T
$\Omega_b h^2$	0.0219	0.0218	0.0219	0.022
$\Omega_{CDM} h^2$	0.1208	0.1222	0.1204	0.1203
100θ	1.041	1.041	1.041	1.041
τ	0.105	0.087	0.089	0.116
α	0.121	0.115	0.162	0.153
$\ln\Delta$	-9.41	-9.4	-9.94	-9.6
n_S	0.9552	0.9478	0.9555	0.9594
r	0.03	0.0002	0.174	0.16
n_T	-	-0.16	-	0.12
k_b	0.0028	0.0028	0.0028	0.0031
$\ln(10^{10} A_S)$	3.08	2.98	2.937	3
Ω_m	0.32	0.33	0.319	0.32
H_0	66.8	66.0	66.9	66.7
$-2\ln\mathcal{L}$ [Best fit]				
commander	-12.11	-12.06	-10.97	-11.12
CAMspec	7794.44	7795.07	7796.84	7794.89
WP	2015.22	2014.91	2013.83	2015.76
BICEP2	-	-	38.79	39.23
Total	9797.55	9797.92	9838.49	9838.76
$-2\Delta\ln\mathcal{L}$	-4.94	-5.04	-11.09	-5.29

This is a good news since it seems by assuming these simple non-power-law forms of the PPS, there will not be any tension between various CMB data and we can still hold on the theoretically important inflationary consistency relation.

Reconstructing inationary potential using BICEP2:

arXiv:1403.5549 30 Mar 2014

S. Choudhury, A. Mazumdar

$$\phi_\star \geq \phi_0 \geq \phi_e$$

VEV

End of inflation

$$V(\phi_0) \ll M_p^4$$

the height of the potential

$$\phi_0 \ll M_p$$

$$|\Delta\phi| \approx |\phi_\star - \phi_e| \ll M_p$$

VEV Variations:

$$0.066 \leq \frac{|\Delta\phi|}{M_p} \leq 0.092.$$

Model independent constraints

The first observable proof of quantum gravity !

$$2.07 \times 10^{16}\ \mathrm{GeV} \leq \sqrt[4]{V_\star} \leq 2.40 \times 10^{16}\ \mathrm{GeV}$$

$$5.27 \times 10^{-9} M_p^4 \leq V(\phi_\star) \leq 9.52 \times 10^{-9} M_p^4,$$
$$2.45 \times 10^{-10} M_p^3 \leq V'(\phi_\star) \leq 1.75 \times 10^{-9} M_p^3,$$
$$4.82 \times 10^{-11} M_p^2 \leq V''(\phi_\star) \leq 6.51 \times 10^{-10} M_p^2,$$
$$6.35 \times 10^{-10} M_p \leq V'''(\phi_\star) \leq 7.56 \times 10^{-10} M_p,$$
$$5.56 \times 10^{-10} \leq V''''(\phi_\star) \leq 4.82 \times 10^{-9},$$

$$5.26 \times 10^{-9} M_p^4 \leq V(\phi_0) \leq 9.50 \times 10^{-9} M_p^4,$$
$$2.44 \times 10^{-10} M_p^3 \leq V'(\phi_0) \leq 1.74 \times 10^{-9} M_p^3,$$
$$4.19 \times 10^{-11} M_p^2 \leq V''(\phi_0) \leq 6.44 \times 10^{-10} M_p^2,$$
$$6.29 \times 10^{-10} M_p \leq V'''(\phi_0) \leq 7.08 \times 10^{-10} M_p,$$
$$5.56 \times 10^{-10} \leq V''''(\phi_0) \leq 4.82 \times 10^{-9},$$

Slow roll Parameters:

$$\epsilon_V \sim \mathcal{O}(0.10 - 1.69) \times 10^{-2},$$
$$|\eta_V| \sim \mathcal{O}(9.14 \times 10^{-3} - 0.06),$$

Some basic conclusions of
Background Imaging of Cosmic Extragalactic Polarization (BICEP2)

1. BICEP2 observations, interpreted most simply, suggest an era of inflation with energy densities of order $(10^{16}\,\mathrm{GeV})^4$, not far below the Planck density $(10^{19}\,\mathrm{GeV})^4$.
2. If the BICEP2 tensor mode results are confirmed by experiments such as PLANCK, confidence in inflationary cosmology will increase significantly.
3. Confirmation of BICEP2 will disfavor large extra dimensions and suggest very high energy densities in the early universe. In fact the existing inflation scenarios in models with large extra dimensions are less appealing than single field scenarios in four dimensions.
4. If the BICEP results prove spurious, the less problematic models of inflation might come back to life.
5. The amplitude of the effect is indeed more or less expected if the scale of Inflation is the scale expected for Grand Unification $(10^{16}\,\mathrm{GeV})^4$.
6. After BICEP2 released its data, many inflation models were investigated in the last few weeks. We believe that it is still too early to say which model is correct.

7. It is interesting to note however, that a proton with boost factor equal to that of a PeV neutrino, PeV /mv ~ 10^16, has an energy of 10^16 GeV, comparable to the Grand Unification scale: arXiv:1404.0622.

The above findings are still preliminary and should not be considered as proved, until they are confirmed by independent experiments like Planck.

Thank YOU